

A Model for Simulation of the Neonatal Lymphatic Transport System

Enhancing our understanding of the neonatal lymphatic (patho)physiology

Carmen den Drijver

Enschede – August 2, 2024

Graduation internship performed at:

**Radboud University Medical Centre Nijmegen, department Neonatology
University of Twente**

Technical Medicine

Medical Sensing and Stimulation

Graduation committee:

Prof. Dr. H.J. Zwart

Professor in Physical Systems and Control, University of Twente

Prof. Dr. W.P. de Boode

Pediatrician-neonatologist, Radboud University Medical Centre Nijmegen

R.J. Lambers MSc

Lecturer Professional Behavior, University of Twente

M.P. Mulder MSc

Technical Physician, University of Twente

Chairman & Technical supervisor

Medical supervisor

Supervisor professional behavior

**Technical Medicine supervisor &
External member**

**UNIVERSITY
OF TWENTE.**

Radboudumc

Abstract

Simulation models can mimic the behavior of physiological systems and therefore assist in clinical decision making. Currently, an explanatory in-silico model of a neonate is being developed at the Amalia Children's Hospital in Nijmegen, called Explain. Our goal was to create a model of the neonatal lymphatic transport system complementary to Explain. We aimed to gain better insight into lymphatic (patho)physiology and the interactions between the lymphatic system and the circulatory and respiratory systems.

The lymphatic model is composed of resistors, capacitances, valves, and time-varying elastances. Capacitances and/or time-varying elastances are connected via resistors or valves. Pressure differences across a resistor or valve generate flow. These pressure differences result from intrinsic and extrinsic pumping. A feedback mechanism model regulates intrinsic pump contraction strength and frequency, which depend on the flow through the lymphatic vessels and the transmural pressure across the lymphatic walls. Parameter values were chosen to achieve target values for interstitial pressure and lymphatic flow under physiological conditions. Two pathological conditions were simulated, namely elevated central venous pressure induced by heart failure and positive pressure ventilation, for validation of the model.

As described in the literature, in our model interstitial fluid is produced due to hydrostatic and osmotic pressure gradients and is taken up by the lymphatic system through extrinsic pumping. Lymph is then propelled through the lymphatic system and returned to the venous circulation via both intrinsic and extrinsic pumping. However, under pathological conditions, lymph production and drainage decreased in the long term, which does not correspond with in vivo measurements.

In conclusion, we have developed a preliminary model representing the physiological lymphatic transport system in neonates. Under pathological conditions, the model's simulations did not fully align with literature reports. Small adaptations to the model have been proposed to resolve these discrepancies. Our modeling effort has provided new insights into the (patho)physiology of the lymphatic system and enhanced our understanding of its interactions with other systems.

Keywords: Lymphatic system, lymphatic flow, thoracic duct flow, neonates, mathematical model, simulation model, positive pressure ventilation (PPV), heart failure, elevated central venous pressure (CVP)

List of abbreviations

CVP	Central venous pressure
ECM	Extracellular matrix
FiO ₂	Fraction of inspired oxygen
HEVs	High endothelial venules
IL	Initial lymphatics
IS	Interstitial space
LD	Lymphatic ducts
LMCs	Lymphatic muscle cells
LT	Lymphatic trunks
LVJ	Lymphovenous junction
PEEP	Positive end-expiratory pressure
PIP	Peak inspiratory pressure
PPV	Positive pressure ventilation
SV	Spontaneous ventilation
SVC	Superior vena cava

Contents

1. Introduction.....	5
2. Background.....	7
2.1 Anatomy	7
2.2 Physiology.....	10
2.3 Pathology.....	14
3. Model Description	15
3.1 Schematic Representation Model	15
3.2 Mathematical Model	17
3.3 Code Implementation.....	23
4. Results	24
4.1 Parameter Estimation	24
4.2 Simulations	24
Discussion.....	33
5.1 Interpretation of the Results	33
5.2 Strengths and Limitations.....	37
5.3 Future Research.....	38
5. Conclusion	39
Appendix A	44
Appendix B	45

1. Introduction

The lymphatic system is a complex and variable network of lymphatic vessels and organs. One of its important functions is removing excess interstitial fluid and returning it to the circulatory system to maintain fluid balance in the body¹. In adults, approximately 8 to 12 liters of interstitial fluid is produced per day². For neonates, this volume is likely even higher when indexed to body weight. Interstitial fluid is drained by the lymphatic system. About two-thirds of the lymph is reabsorbed into the circulatory system via the lymph nodes. The remaining lymph drains into the venous system at the left and right subclavian veins.

When interstitial fluid production exceeds lymphatic drainage or when lymph leaks from the lymphatic vessels, fluid will accumulate. Excessive fluid accumulation in tissues is called tissue edema, while accumulation in serous cavities, such as the pleura, pericardium, or peritoneum, is called pleural effusion, pericardial effusion, or ascites, respectively. Several clinical conditions in neonates may present with edema or effusions, including lymphatic malformations, inflammation, congestive heart failure, and renal failure³. The consequences of edema and effusions vary depending on the cause and location of fluid accumulation. For instance, neonatal pleural effusion can result in respiratory distress⁴. Neonates with chylous ascites, which results from leakage of lipid-rich lymph (chyle) into the peritoneal cavity, typically present with gross abdominal distension, which, if severe, can lead to respiratory compromise⁵. Additional signs may include malabsorption and failure to thrive.

Managing edema and effusions may require the administration of diuretics and/or drainage of lymphatic effusions. Often, edema and effusions resolve once the underlying cause is treated. However, the cause of edema or effusion formation is not always clear, and optimal treatment strategies are sometimes lacking.

The lymphatic system is intricate, and our understanding of its complexities remains limited. Modern imaging techniques, such as dynamic contrast-enhanced magnetic resonance lymphangiography, offer both structural and functional insights into the lymphatic system⁶. However, the exact interactions between the lymphatic system and the circulatory and respiratory systems remain unclear. Lymph flow is influenced by numerous factors including capillary and interstitial hydrostatic and osmotic pressures, contraction strength and frequency of lymphatic muscle cells (LMCs), extrinsic pumping, such as skeletal muscle contractions and fluctuating intrathoracic pressure, lymphatic pressures, and venous pressures. Experimentally measuring and controlling all these parameters in physiological experiments is practically impossible. Therefore, mathematical modeling serves as an important complementary approach to studying the lymphatic system.

Bertram et al.⁷ developed a numerical model of a lymphatic vessel, consisting of a short series chain of contractile segments and inter-segmental valves. They investigated the behavior of chains with one to five contractile segments using pump function curves, with variation of valve opening parameters, maximum contractility, lymphangion size gradation, number of lymphangions, and phase delay between adjacent lymphangion contractions. Passive wall properties were incorporated into the model. Valves were modeled as a resistance that depends on the intralymphatic pressure. They modeled intrinsic contractions as sinusoidal waves immediately following one another, whereas, in reality, a contraction is typically followed by a period of rest. They applied a uniform external pressure to all segments, thus neglecting the influence of varying external pressures depending on location on lymph propulsion. Additionally, they did not incorporate feedback mechanisms such as transmural pressure-dependent and shear stress-dependent contraction frequency and strength. In subsequent studies, Bertram et al. further developed their model by incorporating properties derived from observations and measurements of rat mesenteric vessels⁸. These included a refractory period between contractions, a highly nonlinear form for the passive part of the pressure-diameter relationship, hysteretic and transmural pressure-dependent valve opening and closing pressure thresholds, and dependence of active tension on muscle length as reflected in local diameter. Later,

they implemented a dependency of contraction frequency on transmural pressure. The function for frequency was fitted to experimental data⁹.

Other models for parts of the lymphatic system have been described in the literature. Ikhimwin et al.¹⁰ developed a computational model of a network of initial lymphatics and pre-collectors. Bertram¹¹ created a three-dimensional finite-element fluid/structure-interaction model of an intravascular lymphatic valve. Xie et al.¹² modeled the mechanical feedback mechanisms in a multiscale sliding filament model of lymphatic muscle pumping. However, to the best of my knowledge, no model has been described that represents the entire lymphatic transport system and its interactions with the circulatory and respiratory systems.

This research aims to develop a validated mathematical model of the neonatal lymphatic transport system that interacts with the circulatory and respiratory systems. That can serve as an educational tool and provides new insights into the (patho)physiology of the neonatal lymphatic system and its interactions with other systems. This model will complement Explain, a mathematical model of a neonate developed by Antonius et al.^{13,14} The research question is defined as follows:

Can we create a model of the neonatal lymphatic transport system that can serve as an educational tool for enhancing the understanding of lymphatic (patho)physiology?

To achieve this, the anatomy and physiology of the lymphatic system are described in detail. Additionally, disorders affecting lymphatic flow are briefly discussed. A conceptual model is then developed, which is translated into a mathematical model and implemented in JavaScript. The results include simulations under both physiological and pathological conditions. These simulations are compared with the literature for validation of the model.

2. Background

2.1 Anatomy

The lymphatic system is a complex and variable network of lymphatic vessels and organs. Figure 1 gives a simplified, schematic representation of the lymphatic system. The lymphatic system consists of the initial lymphatic vessels, collecting lymphatic vessels, lymphatic trunks, and lymphatic ducts, as well as primary and secondary lymphatic organs¹⁵.

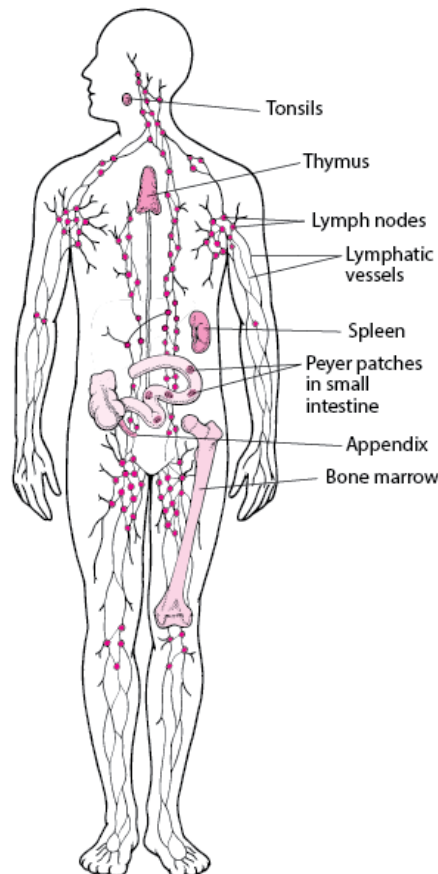


Figure 1: Schematic representation of the lymphatic system with lymphatic vessels and primary and secondary lymphatic organs.⁵⁴

The interstitial space is the space that lies between blood vessels and cells. Fluid is constantly filtered out of the blood capillaries into the interstitial space. Interstitial fluid is removed via lymphatic drainage. In organs located in the pleural, pericardial, and peritoneal spaces, some interstitial fluid filters through the organ's serosal surface into the serous cavity and, then, is also taken up by the lymphatic system¹⁶. Initial lymphatics blindly originate within the interstitial space of vascularized tissues and organs. They consist of a single layer of endothelial cells which are loosely connected through discontinuous button-like junctions (Figure 2), and an incomplete basement membrane¹⁷. The lymphatic endothelial cells have overlapping flaps and are bound to the extracellular matrix of the interstitial space with anchoring filaments. Interstitial pressure will increase secondary to increased interstitial fluid volume, skeletal muscle contraction, or other forces. Under increased interstitial pressures, anchoring filaments pull on the lymphatic endothelial cells and prevent the collapse of the initial lymphatics¹⁸. The parts of the endothelial cells that are not connected to the extracellular matrix by anchoring filaments are bent into the lymphatic lumen, creating pores between the endothelial cells. These pores allow the unidirectional flow of fluid and substances into the initial lymphatics and are referred to as microvalves (Figure 3)¹⁹. A decrease in interstitial pressure, as well as an increase in initial lymphatic pressure, results in the closing of the microvalves. This prevents backflow of fluids from the lymphatic lumen into the interstitial space.

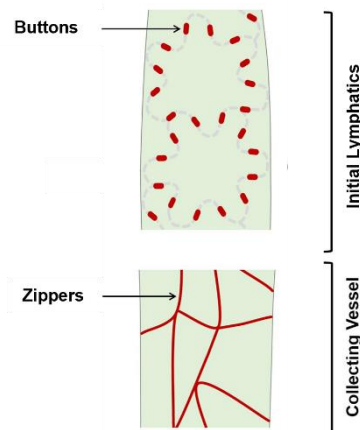


Figure 2: Schematic representation of initial lymphatics with button-like junctions between endothelial cells (upper panel) and collecting lymphatic vessels with zipper-like junctions between endothelial cells (lower panel). Adapted from Zhang et al.¹⁹

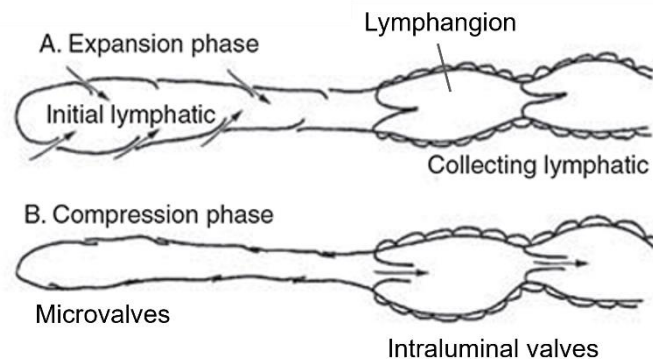


Figure 3: Initial lymphatics with microvalves, and collecting lymphatics with intraluminal valves. The intraluminal vales divide the collecting lymphatic vessels in smaller units, called lymphangions. The arrows represent the direction of lymph flow. (A) During expansion of interstitial fluid volume microvalves open and interstitial fluid flows into the initial lymphatics. (B) Compression closes the microvalves and increase the pressure in the initial lymphatics. As a result of a positive pressure gradient, the intraluminal valves open and lymph flows into the collecting lymphatic vessels.⁵⁵

The initial lymphatic vessels drain into collecting lymphatic vessels. The endothelial cells of the collecting lymphatic vessels are connected through tighter, continuous zipper-like junctions (Figure 2)¹⁷. The collecting lymphatic vessels are covered with LMCs, and have an intact basement membrane^{20,21}. The continuous zipper-like junctions prevent leakage of lymph out of the lymphatic vessels. Collecting lymphatic vessels have intraluminal valves which ensure unidirectional lymph flow (Figure 3)²¹. These intraluminal valves divide the vessels into smaller units, called lymphangions.

Lymph nodes are located along the path of the collecting lymphatics²². Lymph nodes are small bean-shaped structures that consist of multiple lymphoid lobules (Figure 4)²³. Lymph nodes are enclosed by a dense connective tissue capsule. They can be divided into three regions, the cortex, paracortex, and medulla. The space between the capsule and cortex is called the subcapsular sinus and allows the transport of lymph. Afferent lymphatic vessels deliver a constant stream of lymph to the lymph node at the subcapsular sinus. Thereafter, lymph flows through the cortical sinuses and medullary sinus. All lymph drains into a single efferent lymphatic vessel through which it leaves the node. The complex structure of lymph nodes results in a relatively high resistance to flow compared to lymph vessels. Each lymph node is equipped with an artery and vein that provide blood supply and drainage²⁴. Incoming arteries branch into a capillary bed in the cortex of the lymph node which leads directly into the post-capillary venular network where high endothelial venules (HEVs) are located. HEVs merge with larger flat-walled venules in the medulla, which drain into the collecting vein and exit the lymph node. Under homeostatic conditions, HEVs are major portals for the entry of naïve, central memory T and B cells as

well as precursors of conventional dendritic cells, natural killer cells, and plasmacytoid dendritic cells from the bloodstream into the lymph node. Therefore, lymph nodes are an important part of the immune system.

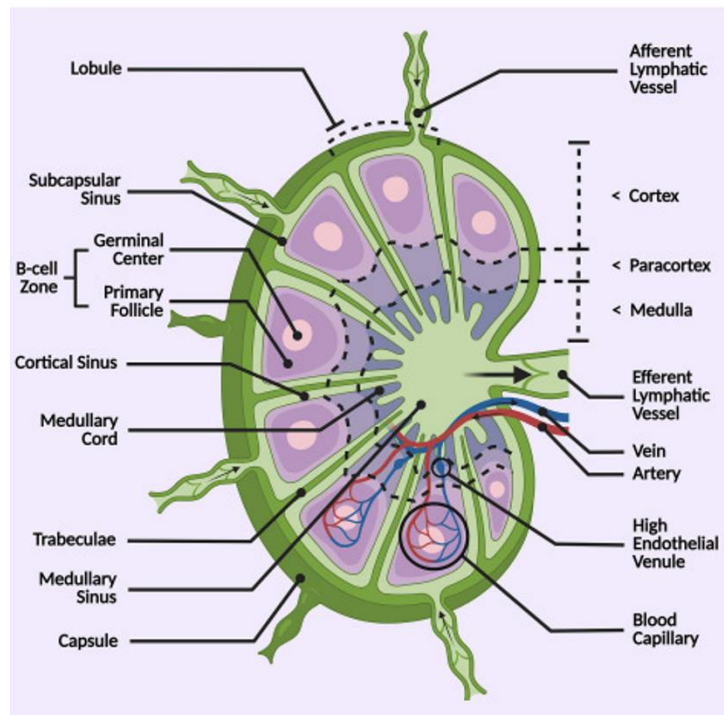


Figure 4: Schematic representation of the lymph node architecture.⁵⁶

Eventually, the efferent collecting lymphatic vessels converge to form larger lymphatic vessels, namely lymphatic trunks and ducts. Lymphatic trunks and ducts also consist of a layer of endothelial cells covered with LMCs and an intact basement membrane. These lymphatic trunks and ducts have intraluminal valves. There are two lymphatic ducts, the right lymphatic duct and the thoracic duct. The right lymphatic duct is located in the right cervical region, just anterior to the anterior scalene muscle¹⁵. It originates at the convergence of the right jugular trunk, right subclavian trunk, and right bronchomediastinal trunk. The right lymphatic duct drains the upper right quadrant of the body and terminates at the junction of the right internal jugular, subclavian, and/or brachiocephalic veins. The thoracic duct drains the rest of the body, namely the left jugular trunk, left subclavian trunk, left bronchomediastinal trunk, left and right lumbar trunks, and intestinal trunk. It originates at the superior aspect of the cisterna chyli, an expanded lymphatic sac at the convergence of the intestinal and lumbar lymphatic trunks around the level of the twelfth thoracic vertebra. The thoracic duct terminates at the junction of the left subclavian and left internal jugular veins. Figure 5 shows the anatomical location of the lymphatic trunks and ducts in the thorax, and the outlet of the lymphatic ducts onto the venous system. At the lymphovenous junction (LVJ), valves prevent blood from refluxing into the lymphatic system²⁵.

Lymphatic organs can be categorized as primary or secondary. Primary lymphatic organs produce lymphocytes and include the bone marrow and thymus¹⁵. Secondary lymphatic organs are sites where the naïve lymphocytes are activated. Secondary lymphatic organs include the spleen, tonsils, lymph nodes, and various mucous membranes such as the Peyer's patches in the intestines.

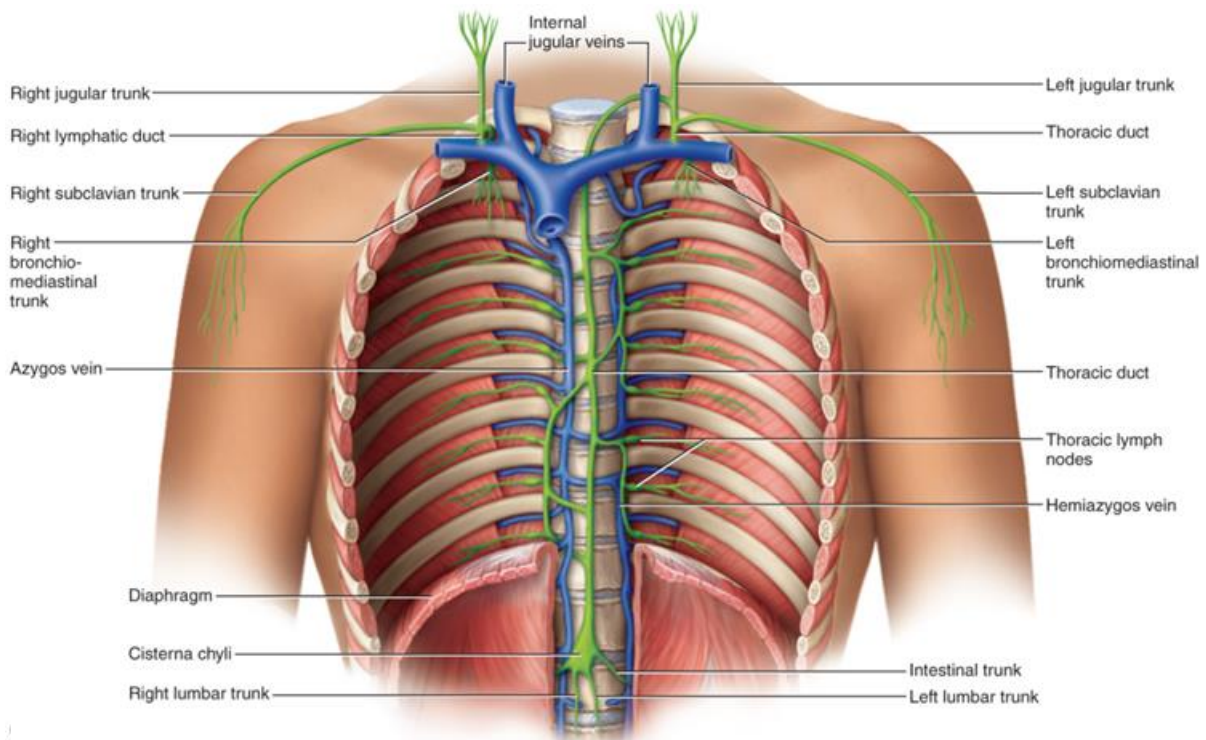


Figure 5: Schematic representation of the anatomical location of the lymphatic trunks and ducts in the thorax, and the outlet of the lymphatic ducts onto the venous system.⁵⁷

2.2 Physiology

The lymphatic system has several functions, it preserves the fluid balance, facilitates the absorption and transportation of dietary fats from the gastrointestinal tract to the bloodstream, and enhances and facilitates the immune system¹. The fluid regulatory function is described below.

Interstitial fluid is formed by transcapillary filtration under hydrostatic and osmotic pressures. Excess interstitial fluid is taken up by the lymphatic system, from then on called lymph, and propelled through the lymphatic vessels and nodes by the intrinsic and extrinsic pump. Intraluminal valves prevent the backflow of lymph. Part of the lymph is reabsorbed by the circulatory system at the lymph nodes due to hydrostatic and osmotic pressure gradients. The remaining lymph is returned to the circulatory system via the thoracic duct and right lymphatic duct.

Transcapillary Filtration

Interstitial fluid is formed by transcapillary filtration, i.e. water and solute transport across the capillary wall²⁶. The transport of water is driven by the hydrostatic and osmotic pressure difference between the blood capillary and the interstitial space. Water flow, f in ml/min, across the capillary wall can be described by the Starling equation:

$$f(t) = L_p S [\Delta p(t) - \sigma \Delta \pi(t)]. \quad (1)$$

Here L_p is the hydraulic conductivity in cm/min·mmHg, describing the permeability of the capillary wall to water. S is the capillary surface area in cm², σ is the osmotic reflection coefficient, and Δp and $\Delta \pi$ are the hydrostatic and osmotic pressure gradients in mmHg, respectively.

Hydrostatic pressure is the pressure exerted by a fluid against the wall of a structure. The hydrostatic pressure depends on the volume of the fluid and compliance of the structure. Under physiologic, non-edematous conditions, the interstitial hydrostatic pressure in tissues such as the skin, intestine, and

lung, is subatmospheric, in the order of -1 to -4 mmHg¹⁶. While in other tissues, including the liver, kidney, and myocardium, the interstitial hydrostatic pressure is normally higher than the atmospheric pressure, around +10 mmHg²⁷. The capillary hydrostatic pressure also varies with anatomical location. Average values at the arteriolar end of the capillaries are +32 to +36 mmHg. Because the fluid encounters resistance along the capillaries, its pressure falls from the arteriolar end to an average of +12 to +25 mmHg at the venule end of the capillaries. Generally, the capillary hydrostatic pressure is higher than the interstitial hydrostatic pressure and is therefore driving fluid out of the capillaries into the interstitial space²⁸.

An increase in interstitial volume results in an increase in interstitial hydrostatic pressure. The degree of the pressure increase depends on the compliance of the wall of the interstitial space¹⁶. Figure 6 represents the general shape of the interstitial pressure-volume relationship in tissues like skin and muscle. At normal to low volumes, the interstitial space has a very low compliance, i.e. a small change in volume results in a large change in interstitial fluid pressure. At higher volumes, the compliance increases, i.e. a large increase in volume results in only a small change in pressure. At excessive increase of interstitial volume, the compliance decreases again due to restriction by fascias²⁹. The increase in compliance with increasing interstitial volume can be attributed to the structural elements of the interstitial space, collectively called the extracellular matrix (ECM). Fibroblasts attach to the collagen fibers of the ECM, and compact the ECM¹⁶. This action, together with the microfibril network of the ECM, acts to reduce interstitial volume and increase interstitial pressure. The glycosaminoglycans of the ECM create an imbibition pressure that acts to expand interstitial volume and decrease interstitial fluid pressure. The interstitial pressure-volume relationship reflects the interaction between these two counterbalancing forces.

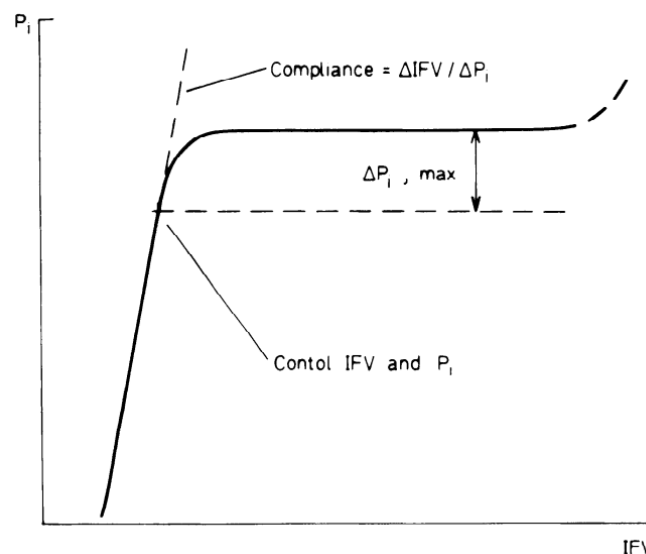


Figure 6: General shape of interstitial pressure-volume relationship. Compliance is constant in dehydration and the initial part of overhydration (linear increase of pressure-volume curve). At further overhydration, compliance increases to infinity (horizontal part of pressure-volume curve). At excessive increase of interstitial fluid volume (IFV), compliance decreases (increase of pressure-volume curve). P_i = interstitial space pressure; $\Delta P_{i,max}$ = maximal rise in P_i that can be obtained as counterpressure toward filtration at overhydration.²⁹

The osmotic gradient is the difference in concentration between two solutions separated by a semipermeable membrane. This concentration difference results in osmosis, i.e. transport of water over the membrane towards the side with the highest concentration solutes. The pressure needed to oppose osmosis is the osmotic pressure. Oncotic pressure, or colloid osmotic pressure, is a type of osmotic pressure induced by plasma proteins, mainly albumin and to a lesser extent globulins, in a body fluid. Normally, the oncotic pressure of plasma is approximately +25 mmHg and does not vary significantly with anatomical location²⁷. The oncotic pressure of the interstitial fluid is dependent on the permeability of the capillaries to plasma proteins, which differs with anatomical location. The

interstitial oncotic pressure is generally lower compared to the plasma oncotic pressure. The interstitial oncotic pressure in the legs is approximately +3 mmHg and in the lungs approximately +18 mmHg. The generally higher capillary oncotic pressure compared to the oncotic pressure in the interstitial space results in net water transport into the capillaries.

Under steady state conditions, there is a slight imbalance in the hydrostatic and oncotic forces acting across the capillary walls, resulting in a net water transport into the interstitial space²¹. This is balanced by the removal of interstitial fluid by the lymphatics.

The transport of solutes across the capillary wall is driven by three mechanisms, namely convective fluid flow, solute diffusion, and transcytosis. In most situations, solute transport across the capillary wall is predominantly driven by convective fluid flow³⁰. When water moves across the capillary wall as a convective flow driven by hydrostatic pressure, solute particles are dragged along irrespective of the solute concentration gradient. Provided that the size of the capillary pores is sufficient to permit passage of the solute, solutes are transported across the capillary wall. Solute particles can also cross the capillary wall through pores by passive diffusion, driven by the solute concentration gradient. Unlike solute transport driven by convective fluid flow and passive diffusion, transcytosis is an active process. Solute particles near the capillary wall are taken up by the endothelial cells into vesicles, transported across their cytoplasm, and released at the other side of the capillary wall²⁷.

Lymph Propulsion

When interstitial fluid enters the initial lymphatics, it is called lymph²¹. Under increased interstitial pressures, the microvalves open, and interstitial fluid enters the initial lymphatics as a result of a pressure gradient. A decrease in interstitial pressure, as well as an increase in initial lymphatic pressure results in the closing of the microvalves which prevents the backflow of fluids from the lymphatic lumen into the interstitial space. Compression of surrounding tissues propels lymph from the initial lymphatics into the collecting lymphatics. Moreover, intrinsic contractions of the collecting lymphatics result in a transient dip in intralymphatic pressure directly after contraction, drawing lymph from the initial lymphatics into the collecting lymphatics³¹. Further propulsion through the lymphatic vessels and nodes occurs through intrinsic pumping, i.e. contraction of the LMCs, and extrinsic pumping, i.e. compression of the lymphatic vessels by surrounding structures, until return to the venous system¹.

Intrinsic Pump

LMCs display both rapid phasic contractions to generate flow, and long-lasting tonic contractions producing constriction to regulate flow¹. Phasic contractions of the LMCs result from rhythmic spontaneous action potentials arising at pacemaker sites located within the muscle layer of the wall of the lymphatic vessels. Action potentials result in a rapid increase in the intracellular calcium concentration which leads to the activation of the muscle regulatory proteins that produce the actin-myosin interactions to contract the muscle cell. Besides contraction activation through pacemaker cells, adrenergic innervation is thought to be involved in intrinsic contraction regulation³². Phasic contraction is essentially uniform within a lymphangion and is usually coordinated with surrounding lymphangions. Functionally, many aspects of lymphatic intrinsic pumping resemble those of cardiac ventricular pumping³³. At the start of a lymphatic pumping cycle, the valves at both ends of the lymphangion are closed so that contraction of the LMCs (i.e. systole) results in a rapid rise in intraluminal pressure. Once the intraluminal pressure exceeds the outflow pressure, the outflow valves open, ejecting lymph. When the LMCs relax (i.e. diastole), intraluminal pressure falls below the outflow pressure, and the outflow valves close. When the intraluminal pressure falls below the inflow pressure, the inflow valves open, allowing lymph to enter the lymphangion. Contraction of a lymphangion takes about two seconds, one second to reduce the diameter of the lymphangion maximally, and one second to return its diameter to the original size¹⁸. Adjacent lymphangions usually contract within 0 to 0.5 seconds of each other, with the most common interval lying between 0 and

0.25 seconds. Contraction frequency and strength are influenced by non-mechanical and mechanical stimuli.

Non-mechanical stimuli include osmolarity of the surrounding interstitial fluid, local tissue temperature, neural and humoral factors, and vasoactive substances. The osmolarity of the interstitial fluid only influences contraction frequency (chronotropic effect), and not contraction strength (inotropic effect)³⁴. Hypoosmolality initially results in an increase in contraction frequency, later followed by a decrease to an almost steady level of about 75% of the frequency in isosmotic conditions. In hyperosmotic conditions, contraction frequency monotonically decreases, in an osmolarity-dependent manner, reaching a steady state. Local tissue temperature affects both contraction frequency and strength. An increase in temperature results in an increase in contraction frequency and a decrease in contraction strength, with a net result of increased flow. The exact effect of neural and humoral factors, and vasoactive substances depends on the specific substance.

Mechanical stimuli include preload, transmural pressure, afterload, and flow. They affect pacemaker activity through pressure-induced vessel stretch and flow-induced shear stress^{12,35}. LMCs exhibit stretch-sensitive calcium release³⁵. Calcium couples to calcium-activated chloride channels, resulting in the efflux of chloride. Together with the influx and efflux of other ions, this results in depolarizations, and when reaching the threshold in an action potential. Increasing the transmural pressure initially results in an increase in contraction strength until a certain threshold. Thereafter, contraction strength decreases with increasing transmural pressure. Contraction frequency increases with increasing transmural pressure. An increased preload, i.e. increased transmural pressure in the preceding lymphangion, results in an increase in both contraction frequency and strength. An increase in afterload, i.e. increased transmural pressure in the next lymphangion, also increases contraction frequency and strength.

Lymph flow induces shear stress, which mediates endothelial production of nitric oxide¹². Elevated nitric oxide in its turn reduces the spontaneous transient depolarizations. Increased flow results in inhibition of the lymphatic pump by decreasing both contraction frequency and strength. This response has been considered as an energy-conserving mechanism for periods when extrinsic (passive) pumping provides sufficient lymph flow. Moreover, under such conditions, intrinsic pumping could be counterproductive, as the phasic constrictions would increase the resistance to flow. The relations between the mechanical stimuli and contraction frequency and strength are shown in Figure 7.

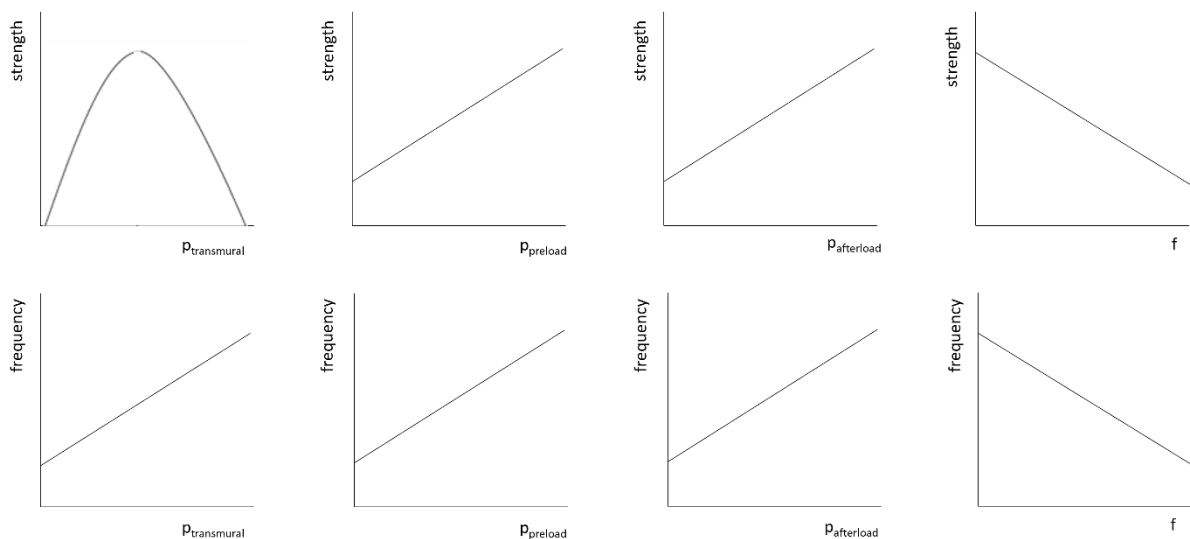


Figure 7: Relation between mechanical stimuli, i.e. transmural pressure ($P_{transmural}$), preload ($P_{preload}$), afterload ($P_{afterload}$) and flow (f), and contraction strength (upper panel) and frequency (lower panel).

The walls of the lymph nodes are also covered with LMCs, thus exhibiting contractile behavior like the lymphatic vessels, although contraction frequency is lower³⁶.

Extrinsic Pump

Extrinsic pumping, i.e. compression of the lymphatic vessels by surrounding structures, originates from contraction of skeletal muscles, arterial pulsations, body movement, respiration, peristalsis, and tissue compression, and results in a complex pressure- and flow pattern³⁷. When the extrinsic pump generates sufficient lymph flow, the intrinsic pump is inhibited. The extrinsic pump is predominant in lymphatics located in tissues undergoing significant cyclic movements³⁴.

Lymph Content

The interstitial fluid contains water, salts, glucose, fatty acids, amino acids, plasma proteins, and white blood cells, just like plasma, and is enriched with products of tissue metabolism and catabolism, apoptotic cells, cell debris, and circulating immune cells³⁸. Because of the high permeability of the initial lymphatics, the composition and solute concentration of pre-nodal lymph is nearly equal to that of interstitial fluid³⁹. Albumin, globulin, and fibrinogen constitute the majority of the lymph proteins, with albumin the major determinant of oncotic pressure. Due to the higher concentration of net negatively charged proteins in the plasma, the concentration cations Na^+ , K^+ , Ca^{2+} , and Mg^{2+} is higher in plasma compared to interstitial fluid⁴⁰. The opposite holds for the concentration anions Cl^- and HCO_3^- , which is higher in interstitial fluid compared to plasma. However, the concentration difference is small. The plasma-protein concentration of pre-nodal lymph is typically below 0.01 g/ml¹⁸. In the lymph nodes, water is reabsorbed by the circulatory system, so that post-nodal lymph has the order of twice the plasma-protein concentration. Post-nodal lymph also has a higher concentration of lymphocytes. Lymph from the intestine and liver is called chyle, it contains between 0.02 and 0.06 g/ml protein and more than 0.01 g/ml triglyceride fat globules which gives it a milky white color.

2.3 Pathology

The lymphatic system regulates the body's fluid balance. Alterations in interstitial fluid production or lymphatic drainage can disturb this balance. When interstitial fluid production exceeds lymphatic drainage, fluid accumulates in tissues and cavities⁴¹. Excessive fluid accumulation in tissue is called edema, and excessive fluid accumulation in a cavity is called an effusion. Edema and effusions can have detrimental effects on tissue function as it increases the diffusion distance for substances²¹. Therefore limiting the supply of oxygen and other nutrients and removal of waste products. Edema and effusions can occur in situations of elevated capillary hydrostatic pressure, lowered plasma oncotic pressure, increased capillary permeability, or alterations in the lymphatic outflow system such as obstruction. Leakage of lymph out of the lymphatic vessels, secondary to trauma or increased lymphatic pressures can also result in effusions. Several safety factors against edema formation exist. An increase in interstitial fluid volume increases interstitial pressure, therefore reducing the hydrostatic pressure gradient between the capillary and interstitial space, and thus reducing transcapillary filtration. Elevated interstitial pressure also favors lymphatic drainage, as the microvalves of the initial lymphatics open under elevated interstitial pressures. Moreover, the interstitial oncotic pressure decreases, as the capillary filtrate is protein-poor, therefore favoring reabsorption by the capillaries. Multiple clinical conditions in neonates may present with edema or effusions, such as congestive heart failure, kidney disease, liver disease, respiratory distress syndrome, malnutrition, malabsorption, and inflammation³. Treatment of the underlying problem will typically resolve the edema and effusions. Lymphatic abnormalities, congenital or acquired, can also result in edema, then called lymphedema, and effusions. Treatment of lymphatic abnormalities is difficult. Most therapies focus on the management of symptoms by reducing interstitial fluid production.

3. Model Description

3.1 Schematic Representation Model

Antonius et al. are developing an in-silico model of a neonate which contains multiple (organ) systems, called Explain¹⁴. In this section, a model of the neonatal lymphatic transport system which interacts with the hemodynamics and ventilation sub-models of Explain is described. Appendix A shows a hydraulic circuit representation of the hemodynamics model of Explain.

Figure 8 shows a schematic representation of the factors influencing the lymphatics model. The lymphatics model responds to the central venous pressure (CVP) and the hydrostatic and oncotic pressures of the hemodynamics model of Explain, the intrathoracic pressure from the ventilation model of Explain, the intrinsic pump elastance and frequency from the feedback mechanism model, and the pressures generated by the extrinsic pump. The lymphatics model reflects lymphatic pressures and flow rates. The feedback mechanism model reflects the characteristics of the intrinsic pump, namely elastance and frequency. The pressures generated by the extrinsic pump are described by functions of time.

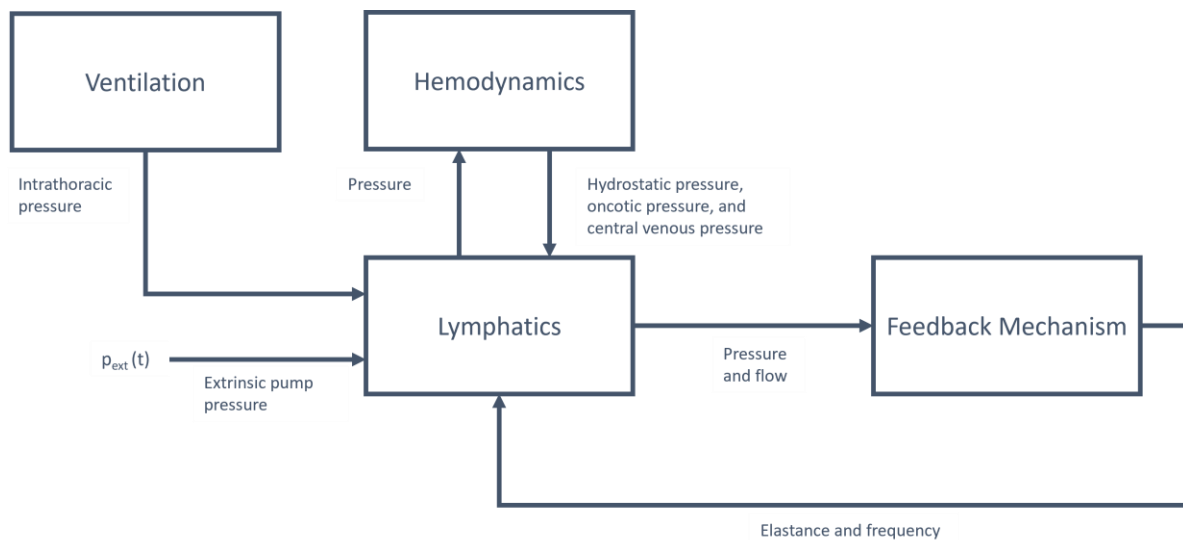


Figure 8: Schematic representation of the factors influencing the lymphatics model.

The lymphatics model is composed of four circuit elements, namely resistors, capacitances, valves, and time-varying elastances, listed in Table 1, relating pressures (p) with flow (f) or volume (v).

Table 1: Circuit elements.

Name	Capacitance	Time-varying elastance	Resistor	Valve
Symbol				

* $p(t)$ = pressure in mmHg; $f(t)$ = flow in ml/min; $v(t)$ = volume in ml.

Figure 9 gives a hydraulic circuit representation of the neonatal lymphatics model with connections to the hemodynamics model of Explain. The components of the hemodynamics model are represented in blue, and the components of the lymphatics model are represented in grey. The compartments, i.e. fluid containing structures, of the lymphatics model include the interstitial space (IS), initial lymphatics (IL), lymphatic trunks (LT), and lymphatic ducts (LD). The IS compartment represents the interstitial space of the whole body. The IL compartment represents all initial lymphatic vessels. The LT compartment represents all collecting lymphatic vessels and all lymphatic trunks, thus the left and right lumbar, jugular, subclavian, and broncho mediastinal trunks, and the intestinal trunk. The LD

compartment represents the thoracic duct and right lymphatic duct. Lymph nodes are not incorporated in this version of the model. The IS and IL are modeled as capacitances. The LT and LD are modeled as time-varying elastances. In the lymphatics model, capacitances and time-varying elastances contain time-varying lymph volumes. Time-varying elastances contain an activation function to simulate contraction. The activation function drives the contraction of the LT and LD by changing the elastance of the compartments over time. All compartments are connected through a resistor or valve. The resistance to transcapillary filtration, i.e. flow from the blood compartments to the IS compartment, is modeled by a resistor. The resistance to flow through microvalves and intraluminal valves, i.e. flow between IS, IL, LT, LD, and SVC (superior vena cava), is modeled by valves. The symbols with a black border represent the intrathoracic components of the models. This distinction allows for the simulation of the effects of intrathoracic pressure, from the ventilation model, on the lymphatic circulation. The arrows represent the direction of fluid flow under physiological conditions, which is referred to as forward flow.

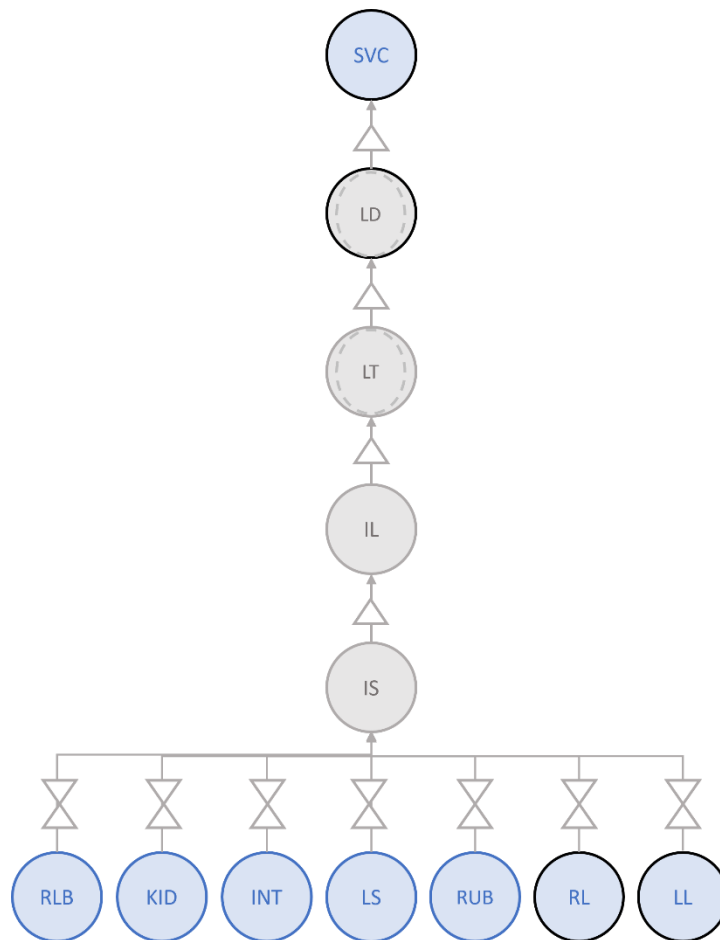


Figure 9: Hydraulic circuit representation of the neonatal lymphatics model (symbols in blue) with connections to the hemodynamics model (symbols in grey). RLB = remainder lower body; KID = kidneys; INT = intestines; LS = liver and spleen; RUB = remainder upper body; RL = right lung; LL = left lung; IS = interstitial space; IL = initial lymphatics; LT = lymphatic trunks; LD = lymphatic ducts; SVC = superior vena cava.

The feedback mechanism model responds to the flow between the LD and SVC, and the transmural pressure across the wall of the LD. It determines the control effector minute-elastance. Minute-elastance is the product of the maximum increase in elastance during intrinsic contraction and intrinsic contraction frequency, which are sent to the lymphatics model. Relationships between the input and output variables of the feedback mechanism model are based on the Wesseling and Settels baroreflex model with simplified linear characteristics as described by van Meurs^{42,43}. Activation functions $a(cv)$ of the controlled variables (cv), flow and transmural pressure, consist of an active part in the range $[CV_{min}, CV_{max}]$, see Figure 10. Below CV_{min} and above CV_{max} the effect of the controlled variable saturates. In

the setpoint CV_{sp} , the output of the function is zero. CV_{min} and CV_{max} are not necessarily symmetrical around CV_{sp} , allowing for the representation of multiple controlled variables with the same model. The output of the activation function passes through a filter mimicking response times. The output of the filter is then multiplied by control gains for changes to the control effector from its reference value. The gain can be positive, zero, or negative. The latter is the case for the effect of flow on E_{amp} and frequency, resulting in a decrease of E_{amp} and frequency in response to a rise in flow. For the controlled variable transmural pressure, the gain is positive, resulting in an increase of E_{amp} and frequency in response to a rise in transmural pressure. This setup results in zero deviation from the control effector reference value when the controlled variables are in their setpoints. The influence of non-mechanical stimuli, preload, and afterload on the intrinsic pump are not implemented in the model.

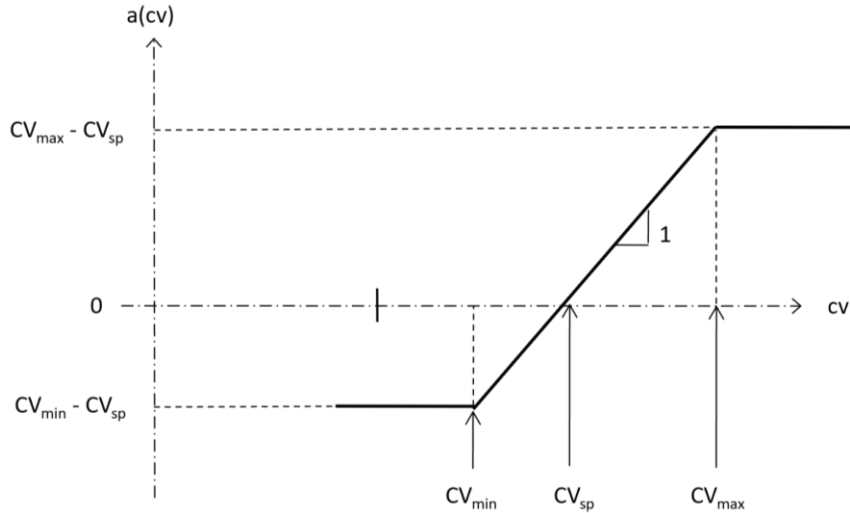


Figure 10: Activation function $a(cv)$. cv = controlled variable; CV_{min} = value of controlled variable below which the output of the activation function is constant; CV_{max} = value of controlled variable above which the output of the activation function is constant; CV_{sp} = value of the controlled variable at which the output of the activation function is zero.⁴³

3.2 Mathematical Model

The circuit elements of the lymphatics model are listed in Table 1. The IS and IL compartments of the lymphatics model are modeled as capacitances. The pressure in a capacitance is modeled by:

$$p_j(t) = E_j[v_j(t) - UV_j] + p_{ext_j}(t), \quad (2)$$

where E_j is the elastance in mmHg/ml, v_j is the volume in ml and UV_j is the unstressed volume in ml, of capacitance j . p_{ext_j} is the pressure, in mmHg, acting on capacitance j from the outside, i.e. extrinsic pump pressure. The pressure inside a capacitance will change as a result of a change in volume or extrinsic pump pressure. Capacitances show a linear behavior between volume and transmural pressure, i.e. the pressure difference between the inside and outside of a structure. When the pressure in the capacitance is equal to the extrinsic pump pressure, the volume is equal to its unstressed volume.

The LT and LD compartments of the lymphatics model are modeled as time-varying elastances. Time-varying elastances contain an activation function that temporarily increases the elastance over time. Such a temporary increase in elastance simulates an intrinsic contraction. The pressure inside a time-varying elastance changes secondary to a change in volume or extrinsic pump pressure, or as a result of a change in elastance. The pressure in a time-varying elastance is modeled similarly as the pressure in a capacitance:

$$p_j(t) = E_j(cv, t)[v_j(t) - UV_j] + p_{ext_j}(t). \quad (3)$$

The elastance E_j varies over time, and is modeled by:

$$E_j(cv, t) = E_{min} + E_{amp}(cv) \cdot M(t), \quad (4)$$

where E_{min} is the minimum elastance, E_{amp} is the maximum increase elastance during intrinsic contraction, in the model also referred to as contraction strength, both in mmHg/ml, of time-varying elastance j . E_{amp} comes from the feedback mechanism model. $M(t)$ is the contraction activation function, which varies between 0 and 1 (dimensionless). $M(t)$ is modeled by, from Bertram et al.⁴⁴:

$$M(t) = \begin{cases} 0.5 \left[1 - \cos\left(\frac{2\pi}{T_c}[t - t_s]\right) \right], & t_s \leq t \leq t_s + T_c \\ 0, & t_s + T_c < t < t_{s_{new}} \end{cases} \quad (5)$$

The waveform of contraction activation is a smooth curve that rises till 1 and symmetrically declines to 0 between the times $t = t_s$ and $t = t_s + T_c$ (Figure 11). Here, t_s is the time at the beginning of a contraction, and T_c is the duration of the contraction, both in minutes. The relaxation phase starts at $t = t_s + T_c$. The duration of the relaxation phase, T_r in minutes, is calculated by:

$$T_r(freq) = \frac{1}{freq(cv)} - T_c, \quad (6)$$

where $freq$ is the contraction frequency in min^{-1} . As $T_r \geq 0$, $freq \leq \frac{1}{T_c}$. $freq$ comes from the feedback mechanism model. During relaxation, $M(t)$ equals zero, $E_j = E_{min}$, and the time-varying elastance resembles a capacitance. $t_{s_{new}}$ is the time at the beginning of the next contraction, in minutes:

$$t_{s_{new}} = t_s + \frac{1}{freq(cv)}. \quad (7)$$

After one cycle, i.e. a period of contraction followed by a period of relaxation, the cycle is repeated, where $t_{s_{new}}$ becomes t_s .

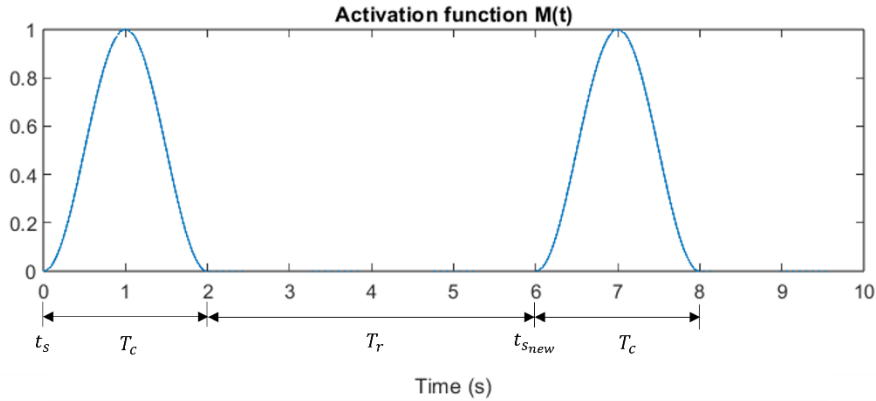


Figure 11: Activation function $M(t)$ of the intrinsic pump. t_s = time at the beginning of a contraction; $t_{s_{new}}$ = time at the beginning of the next contraction; T_c = duration of a contraction; T_r = duration of the relaxation phase. Here $T_c = 2$ s and $T_r = 4$ s.

Fluid flow between capacitances and time-varying elastances results from pressure gradients. The IS and IL, IL and LT, LT and LD, and LD and SVC are connected via valves. The flow across a valve is modeled by:

$$f_{j,k}(t) = \begin{cases} \frac{p_j(t) - p_k(t)}{R_{j,k}}, & p_j(t) > p_k(t) \\ 0, & p_j(t) \leq p_k(t) \end{cases} \quad (8)$$

Here $f_{j,k}$ is the flow in ml/min, and $R_{j,k}$ is the valve resistance in mmHg·min/ml, between capacitances and/or time-varying elastances j and k . The valves are modeled as perfect valves, i.e. the resistance to retrograde flow is infinite. Therefore, only forward flow is possible. Valves show a linear relationship between flow and transvalvular pressure, i.e. pressure difference between both sides of the valve.

The blood capacitances of the hemodynamics model, RLB, KID, INT, LS, RUB, RL and LL, are connected to the IS of the lymphatics model via resistors. The flow across a resistor, is modeled by:

$$f_{j,k}(t) = L_p S [\Delta p(t) - \sigma \Delta \pi]. \quad (9)$$

Here L_p is the hydraulic conductivity in cm/min·mmHg, describing the leakiness of the capillary wall to water. S is the capillary surface area in cm², σ is the osmotic reflection coefficient which is dimensionless, and Δp and $\Delta \pi$ are the hydrostatic and osmotic pressure differences in mmHg, respectively.

The hydrostatic pressure, p , in a capacitance, is modeled by Equation 2. The hydrostatic pressure difference, Δp , can be calculated by:

$$\Delta p(t) = p_j(t) - p_k(t). \quad (10)$$

Here j is a blood capacitance from the hemodynamics model, k the lymph capacitance IS from the lymphatics model.

The osmotic pressure, π , inside a capacitance, in mmHg, is modeled by:

$$\pi = iMRT, \quad (11)$$

where i is the van 't Hoff factor, M is the molar concentration of the solution in mmol/ml, R is the ideal gas constant in ml·mmHg/mmol·K, and T is the temperature in K. M and T are assumed to be constant over time.

The osmotic pressure difference, $\Delta \pi$, can be calculated by:

$$\Delta \pi = \pi_j - \pi_k. \quad (12)$$

Here j is a blood capacitance from the hemodynamics model, k the lymph capacitance IS from the lymphatics model.

Equation 9 can be rewritten in the same form as Equation 8:

$$f_{j,k}(t) = \frac{p_j(t) - p_k(t)}{R_p} - \frac{\pi_j - \pi_k}{R_\pi}, \quad (13)$$

with

$$R_p = \frac{1}{L_p \cdot S}, \quad (14)$$

and

$$R_\pi = \frac{1}{L_p \cdot S \cdot \sigma}. \quad (15)$$

The first term describes the flow resulting from a hydrostatic pressure gradient. The second term describes the flow resulting from an osmotic pressure gradient. R_p is the resistance of the capillary wall to water transport due to a hydrostatic pressure gradient, in mmHg·min/ml. R_π is the resistance of the capillary wall to water transport due to an osmotic pressure gradient, in mmHg·min/ml. Flow across a resistor can occur in two directions, and the resistance to flow is equal in both directions.

The volume change, in L, of compartment j can be calculated by adding all flow rates:

$$\frac{\Delta v_j(t)}{\Delta t} = f_{in}(t) - f_{out}(t), \quad (16)$$

where f_{in} is the sum of all flow rates entering compartment j , and f_{out} the sum of all flow rates leaving compartment j .

Figure 12 shows a block diagram of the feedback mechanism model and its interaction with the lymphatics model. The feedback mechanism model changes intrinsic contraction strength, E_{amp} , and intrinsic contraction frequency, $freq$, based on the controlled variables (cv) flow ($f_{LD,SVC}$) and transmural pressure ($p_{tm_{LD}}$), to compensate for changes in extrinsic pumping.

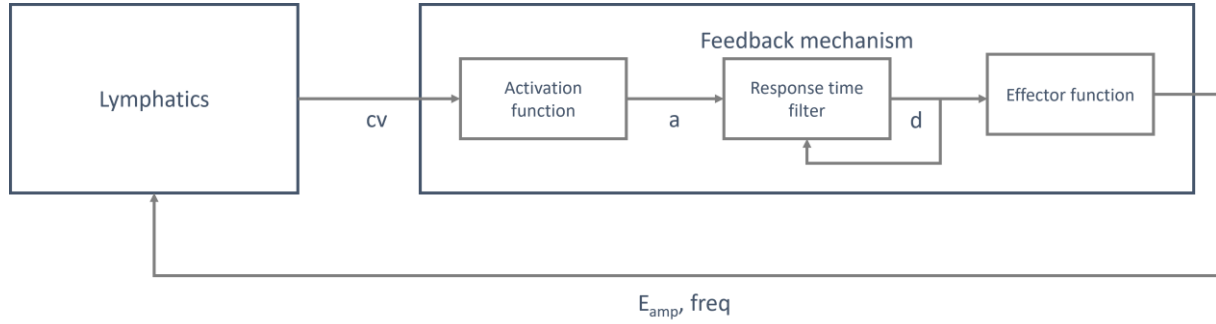


Figure 12: Block diagram of the feedback mechanism model and its interaction with the lymphatics model. cv = controlled variable; a = activation; d = filtered activation; E_{amp} = maximum increase in elastance during intrinsic contraction; $freq$ = contraction frequency.

The feedback mechanism model is based on the activation function from van Meurs⁴³, shown in Figure 10. The activation function $a(cv)$ for controlled variable cv is described by:

$$a(cv) = \begin{cases} CV_{min} - CV_{sp}, & cv \leq CV_{min} \\ cv - CV_{sp}, & CV_{min} < cv < CV_{max} \\ CV_{max} - CV_{sp}, & cv \geq CV_{max} \end{cases} \quad (17)$$

a is the activation in ml/min and mmHg for flow and pressure respectively. CV_{min} is the value of the controlled variable below which the effect of the controlled variable saturates, the output of the activation function is minimal. CV_{max} is the value of the controlled variable above which the effect of the controlled variable saturates, the output of the activation function is maximal. CV_{sp} is the value of the controlled variable at which the output of the activation function is zero. When the controlled variable is equal to CV_{sp} , the control effector is equal to its reference value.

The activation is filtered by a response time filter. d is the filtered activation secondary to the controlled variable flow ($f_{LD,SVC}$) or transmural pressure ($p_{tm_{LD}}$), in ml/min and mmHg, respectively. The change in d is described by:

$$\frac{\Delta d}{\Delta t} = \frac{1}{t_c} [a(cv) - d(cv)], \quad (18)$$

where tc is the time constant in minutes. d strives to become equal to a . The tc makes sure that d is not immediately changed to a but is changed gradually.

E_{amp} and $freq$ are derived from the control effector minute-elasticance:

$$me(cv) = E_{amp}(cv) \cdot freq(cv). \quad (19)$$

The control effector minute-elasticance, me , in mmHg/ml·min, depends on the controlled variables flow ($f_{LD,SVC}$) and transmural pressure ($p_{tm,LD}$), and is modeled by:

$$me(d_f, d_{p_{tm}}) = me_{ref} + [d_f(f_{LD,SVC}) \cdot g_f] + [d_{p_{tm}}(p_{tm,LD}) \cdot g_{p_{tm}}], \quad (20)$$

with

$$g_f = \begin{cases} g_{f,low}, & a(f) \leq 0 \\ g_{f,high}, & a(f) > 0 \end{cases}$$

and

$$g_{p_{tm}} = \begin{cases} g_{p_{tm},low}, & a(p_{tm}) \leq 0 \\ g_{p_{tm},high}, & a(p_{tm}) > 0 \end{cases}$$

me_{ref} is the reference value of the control effector minute-elasticance, i.e. the minute-elasticance at which the controlled variables are in their setpoints during steady state under physiological conditions, in mmHg/ml·min. g_f and $g_{p_{tm}}$ are the gains in mmHg/ml² and ml⁻¹·min⁻¹ for flow and transmural pressure respectively. The lower gains, $g_{f,low}$ and $g_{p_{tm},low}$, were chosen such that me reaches a maximum value when the controlled variables, flow and transmural pressure respectively, are smaller or equal to CV_{min} . The higher gains, $g_{f,high}$ and $g_{p_{tm},high}$, were chosen such that me is almost zero when the controlled variables, flow and transmural pressure respectively, are larger or equal to CV_{max} .

The maximum increase in elasticance during intrinsic contraction, E_{amp} , and intrinsic contraction frequency, $freq$, are derived from the control effector minute-elasticance:

$$freq(me) = \sqrt{me(d_f, d_{p_{tm}})/R}, \quad (21)$$

and

$$E_{amp} = me(d_f, d_{p_{tm}})/freq, \quad (22)$$

where R is the ratio, in mmHg·min/ml between frequency and elasticance. Therefore,

$$E_{amp} = freq \cdot R. \quad (23)$$

R is assumed to be constant. E_{amp} and $freq$ are inputs to the lymphatics model.

The extrinsic pump pressure $p_{ext,j}(t)$, i.e. the pressure generated by the extrinsic pump, acting on the IL, LT, and LD, is an input to the lymphatics model. The extrinsic pump pressure is different for the

different compartments of the lymphatics model. In the model, there is no extrinsic pump pressure that acts on the IS. The extrinsic pump pressure acting on the IL is described by:

$$p_{ext,IL}(t) = A[b - \cos(2\pi ft)], \quad (24)$$

with A the amplitude of the waveform in mmHg, f the frequency of the waveform in min^{-1} , and t the time in minutes. $A \cdot b$ is the value around which the sine fluctuates. b is a dimensionless value between -1 and 1. $p_{ext,IL}$ describes the sinusoidal variation of the extrinsic pump pressure which varies between $A \cdot b - A$ and $A \cdot b + A$, with frequency f , see Figure 13. The negative parts of the curve simulate the pulling on the anchoring filaments which lowers the pressure in the initial lymphatics. The positive parts of the curve simulate compression of the initial lymphatics by surrounding structures, which increases the pressure in the initial lymphatics. Sinusoidal variation is a simplification, as the external pressure varies more randomly over time.

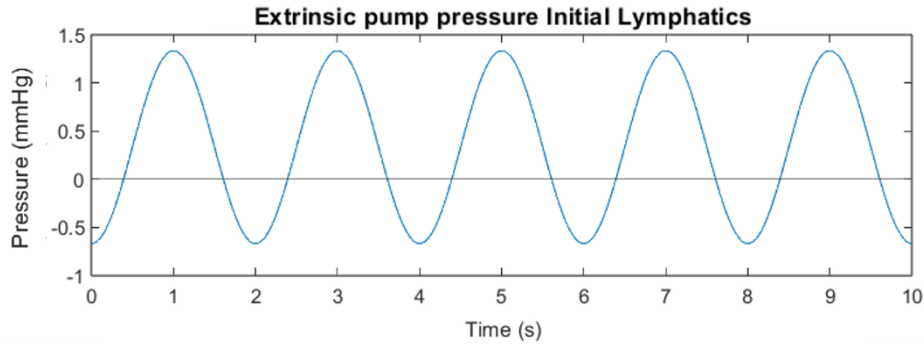


Figure 13: Extrinsic pump pressure acting on the initial lymphatics. Here $A = 1$ mmHg, $b = 1/3$, and $f = 0.5 \text{ sec}^{-1}$.

The extrinsic pump pressure acting on the LT is described by:

$$p_{ext,LT}(t) = \begin{cases} \frac{1}{2} \cdot A \left[1 - \cos\left(\frac{2\pi}{T_c}[t - t_s]\right) \right], & t_s \leq t \leq t_s + T_c \\ 0, & t_s + T_c < t < t_{s_{new}} \end{cases} \quad (25)$$

The waveform of the extrinsic pump pressure is a smooth curve that rises till A and symmetrically declines to 0 between the times $t = t_s$ and $t = t_s + T_c$, see Figure 14. Here, t_s is the time at the beginning of a compression and T_c is the duration of the compression in minutes. A period of relaxation, starts at $t = t_s + T_c$.

The duration of the period of relaxation, in minutes, is calculated by:

$$T_r = \frac{1}{freq} - T_c, \quad (26)$$

where $freq$ is the contraction frequency in min^{-1} .

$t_{s_{new}}$ is the time at the beginning of the next contraction:

$$t_{s_{new}} = t_s + \frac{1}{freq}. \quad (27)$$

After one cycle of contraction followed by a period of relaxation, the cycle is repeated where $t_{s_{new}}$ becomes t_s . Simulation of the extrinsic pump pressure by $p_{ext,LT}$ is again a simplification.

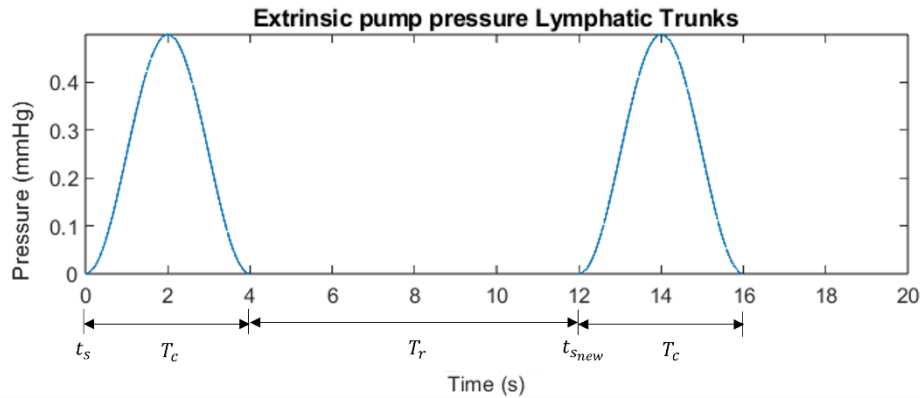


Figure 14: Extrinsic pump pressure acting on lymphatic trunks. t_s = time at the beginning of a contraction; T_c = duration of a contraction; T_r = duration of relaxation period. Here $A = 0.5$ mmHg, $T_c = 4$ sec, $T_r = 8$ sec.

Extrinsic pumping of the thoracic duct results from arterial pulsations and respiration. Therefore, the extrinsic pump pressure acting on the LD, $p_{ext,LD}$, is equal to the intrathoracic pressure from the ventilation model of Explain.

All pressures in the lymphatics model, are relative to the atmospheric pressure, p_{Atm} (p_{Atm} is said to be zero).

Summarizing, the model is composed of resistors, capacitances, valves and, time-varying elastances. Capacitances and/or time-varying elastances are connected via a resistor or valve. Pressure differences across a resistor or valve generate flow. These pressure differences result from intrinsic and extrinsic pumping. The feedback mechanism model regulates intrinsic pumping by changing the maximum increase in elastance of the LT and LD of the lymphatics model and the frequency of the contractions. These variables depend on the flow through the LD and the transmural pressure of the LD. When flow and transmural pressure are smaller than CV_{min} or larger than CV_{max} , the effect on the control effector saturates.

3.3 Code Implementation

The model code is available via: <https://github.com/Dobutamine/explain-web/tree/carmen>. The baseline_neonate.json file, accessed via 'public/model_definitions', contains all components of the model. Each component of which the model type starts with 'Lymph' was added to the file. All settings, thus enabled components and parameter values as in the file, apply to the physiological situation. The description of the model types can be accessed via 'src/explain/core_models'.

4. Results

4.1 Parameter Estimation

The hemodynamics and ventilatory model of Explain contain many parameters that are already estimated by Antonius et al. It was chosen to keep these parameter values unchanged. The parameter values for the components of the lymphatics model were chosen to obtain a mean forward flow between the LD and SVC (LD outflow) of 0.14 ml/kg/min, and a mean pressure in the IS of -3.4 mmHg under physiological conditions. These target values are derived from the literature as described below.

Lymph flow through the thoracic duct towards the venous system in adults is estimated to be 1.38 ml/kg/hour⁴⁵. Animal studies showed that lymphatic flow in the fetus and neonate is approximately five times higher compared to the adult when corrected for body weight⁴⁶. Based on these values the flow through the thoracic duct in a neonate can be estimated, which results in a flow of 6.9 ml/kg/hour. Leeds et al. measured the lymph flow through the thoracic duct and right lymphatic duct in dogs. They found a flow of 18.5 ml/hour and 3.5 ml/hour in the thoracic and right lymphatic ducts, respectively⁴⁷. Therefore, about 5/6th of the total lymph drains via the thoracic duct into the central venous system, and 1/6th drains via the right lymphatic duct into the central venous system. The total lymph flow through the thoracic duct and right lymphatic duct is therefore estimated to be 8.28 ml/kg/hour, which is approximately 0.14 ml/kg/min.

As the intestines are responsible for a great part of the lymph production the target value for IS pressure is chosen to be -3.4 mmHg¹⁶.

Parameter values for the physiological situation are presented in Appendix B. Initially parameter values were chosen based on values used in the hemodynamics model or the literature. The values were changed based on simulations until the desired target values for IS pressure and LD outflow were reached.

4.2 Simulations

Physiological situation

Figure 15 shows the pressures inside the IS, IL, LT, LD, and SVC under physiological conditions during steady state, meaning that LD outflow is equal to IS inflow. During steady state, LD outflow is 0.14 ml/kg/min, and mean IS pressure is -3.4 mmHg, see Appendix B for the parameter values under physiological conditions.

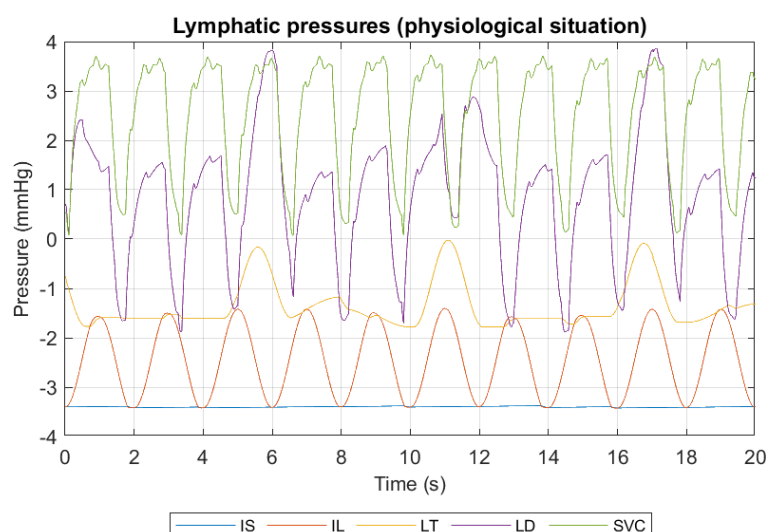


Figure 15: Lymphatic pressures under physiological conditions. IS = interstitial space; IL = initial lymphatics; LT = lymphatic trunks; LD = lymphatic ducts; SVC = superior vena cava.

The pressure in the IS is approximately constant. The small changes in IS pressure are secondary to volume changes due to the filling and draining of the IS. IL pressure shows a variation that looks like a sinusoid. This is the result of the extrinsic pump pressure that acts on the IL, which is modeled as a sinusoidal function, see Equation 24. The minima and maxima of the IL pressure curve vary as a result of volume changes due to the filling and draining of the IL. The transient increases in LT pressure are due to intrinsic (higher peaks) and extrinsic (lower peak) pumping of the LT. The amplitude of the peaks and distance between the peaks (frequency) secondary to intrinsic contractions vary, depending on the transmural pressure across the wall of the LD and the outflow of the LD, modeled by the feedback mechanism model (Equations 17-23). The amplitude also depends on the volume of the LT. The pressure increases secondary to extrinsic pumping occur at a constant frequency. Extrinsic pumping is modeled as a sinusoid with a constant amplitude, see Equation 25. The small changes in LT pressure are the result of volume changes due to the filling and drainage of the LT. The pressure in the LD changes due to intrinsic and extrinsic pumping of the LD. Extrinsic pumping of the LD is the result of intrathoracic pressure changes, which are mainly due to respiration, modeled by the ventilation model of Explain. Inspiration lowers LD pressure, expiration increases LD pressure. Intrinsic contractions increase LD pressure with varying amplitude and frequency, depending on the transmural pressure across the wall of the LD and the outflow of the LD, modeled by the feedback mechanism model. The pressure in the SVC also changes secondary to intrathoracic pressure changes, as well as volume changes due to the filling and draining of the SVC. From the IS towards the SVC, the mean pressure increases.

In the model, the valves only allow forward flow, see Equation 8. Therefore, flow between two compartments occurs when the pressure in a compartment becomes higher than the pressure in the next compartment. Thus, flow from the IS to the IL is secondary to the extrinsic pumping of the IL. Flow from the IL to the LT is also secondary to extrinsic pumping of the IL. Flow from the LT to the LD is secondary to respiration, specifically inspiration. Intrinsic and extrinsic pumping of the LT aid lymph flow when a contraction or compression coincides with inspiration. Flow from the LD to the SVC is secondary to intrinsic contractions of the LD. Lymph flow between the compartments in the model is not constant and has a pulsatile pattern, as can be seen in Figure 16.

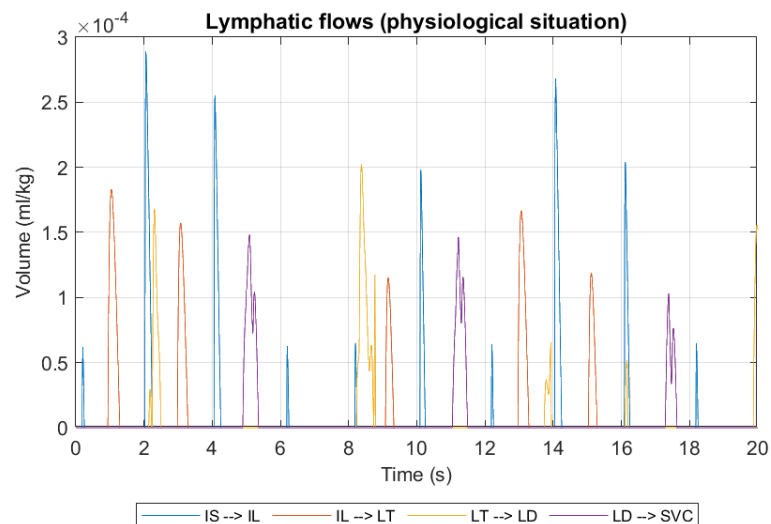


Figure 16: Instantaneous flow between the IS and IL, IL and LT, LT and LD and LD and SVC. IS = interstitial space; IL = initial lymphatics; LT = lymphatic trunks; LD = lymphatic ducts; SVC = superior vena cava.

Elevated central venous pressure

The influence of an elevated CVP on interstitial fluid production and lymph drainage in the model was investigated. To obtain an elevated CVP, the maximum elastance, i.e. contraction strength, of the ventricles was lowered to 50% of its original value.

Right and left ventricular stroke volume decreased and the heart rate increased compared to the physiological situation. Together this led to a decrease in cardiac output. The pressure changes in the blood-containing compartments of the hemodynamics model of Explain (see Appendix A) secondary to a decrease in contraction strength of the ventricles, compared to the physiological situation, are presented in Table 2. The pressure in the ventricles (RV and LV) is decreased, and the pressure in the atria (RA and LA) is increased. The pressure in the arterial system (AA, AAR, AD, and PA) is decreased. The pressure in the capillary system (BR, RUB, LS, INT, KID, RLB, RL, and LL) is also decreased, except for the pressure in COR, which is increased. The pressure in the venous system (IVCE, IVCI, SVC, and PV) is increased.

Table 2: Pressure change in the blood containing compartments of Explain secondary to a decrease in ventricular contraction strength compared to the physiological situation.

	LL	PV	LA	LV	AA	AAR	AD
Pressure change compared to physiological situation	↓	↑	↑	↓	↓	↓	↓
	COR	BR	RUB	LS	INT	KID	RLB
	↑	↓	↓	↓	↓	↓	↓
	IVCE	IVCI	SVC	RA	RV	PA	RL
	↑	↑	↑	↑	↓	↓	↓

* LL = left lung; PV = pulmonary vein; LA = left atrium; LV = left ventricle; AA = ascending aorta; AAR = aortic arch; AD = descending aorta; COR = coronary arteries; BR = brain; RUB = remainder upper body; LS = liver and spleen; INT = intestines; KID = kidneys; RLB = remainder lower body; IVCE = extra-thoracic inferior vena cava; IVCI = intrathoracic inferior vena cava; SVC = superior vena cava; RA = right atrium; RV = right ventricle; PA = pulmonary artery; RL = right lung.

Figure 17 a shows the pressure in the IS, IL, LT, LD, and SVC. The first 20 seconds represent the pressures under physiological conditions. After 20 seconds (dotted line), the contractility of the ventricles is lowered. It can be seen that from that point, the pressure in the SVC gradually increases. Figure 17 b shows the pressures 8 minutes after the ventricular contraction strength was decreased, the mean pressures are approximately constant, and a new steady state is reached. It can be seen that the pressure in the IS, IL, LT, and LD have increased compared to Figure 17 a. The pressure increases secondary to intrinsic contractions (higher peaks) have a varying amplitude.

Lymph flow between the compartments is a result of the same intrinsic and extrinsic pump pressures as for the physiological situation.

Table 3 presents the mean IS inflow, mean LD outflow and mean IS pressure under physiological conditions, and at 1 and 8 minutes after the contraction strength of the ventricles was lowered. IS inflow slightly decreases secondary to a decreased ventricular contraction strength. One minute after the onset of a decreased contractility, the outflow of the LD is lower than the inflow of the IS, and IS pressure has increased compared to the physiological situation. After 8 minutes, a new steady state is reached, IS inflow and LD outflow are equal. In the new steady state, these flows are slightly lower compared to the physiological situation. IS pressure has further increased.

Positive Pressure Ventilation (PPV)

The influence of PPV on interstitial fluid production and lymph drainage in the model was investigated. For the simulations with PPV, the mechanical ventilator was enabled in the model and spontaneous ventilation (SV) was switched off. The type of PPV was pressure-controlled ventilation. The ventilator settings were as follows: peak inspiratory pressure (PIP) 10.30 mmHg (14 cmH₂O), positive-end

expiratory pressure (PEEP) 2.21 mmHg (3 cmH₂O), respiration frequency 40/min, inspiration time 0.4 sec, flow 12 l/min, fraction of inspiratory oxygen (FiO₂) 0.21.

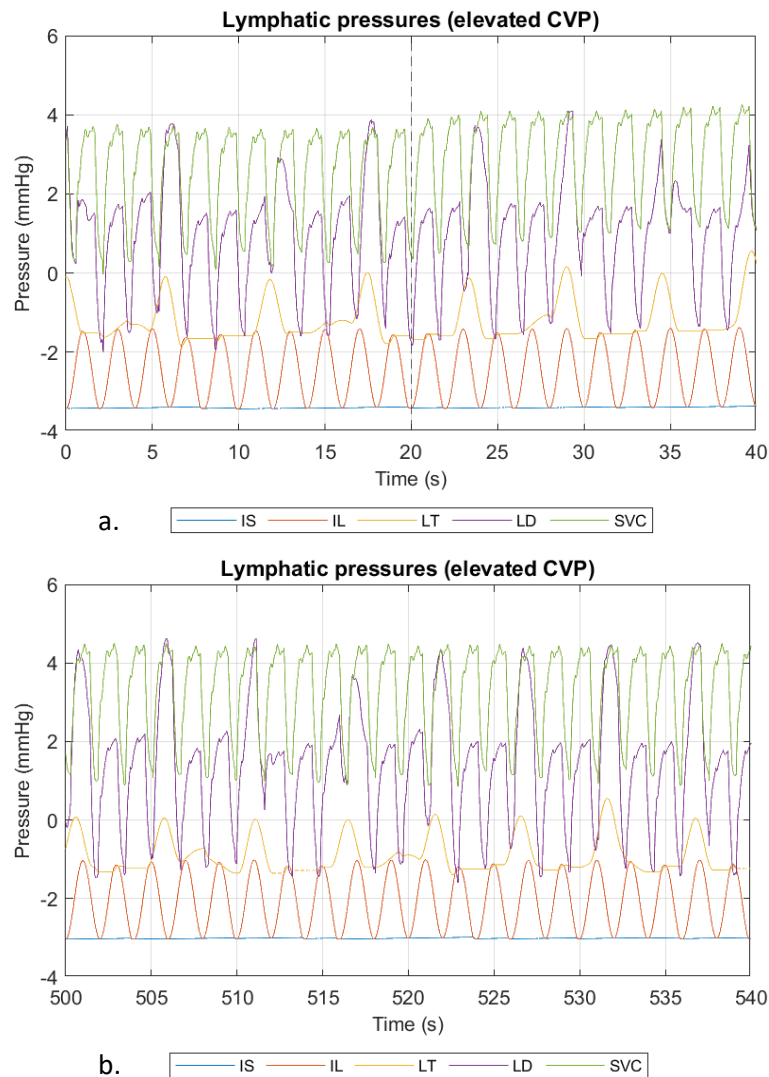


Figure 17: Lymphatic pressures. The dotted line in figure a marks the onset of a decreased ventricular contraction strength. Figure b shows the pressures 8 minutes after the onset of a decreased ventricular contraction strength. IS = interstitial space; IL = initial lymphatics; LT = lymphatic trunks; LD = lymphatic ducts; SVC = superior vena cava.

Table 3: IS inflow, LD outflow and IS pressure under physiological conditions and during a decreased ventricular contraction strength.

	Physiological situation	Decreased ventricular contraction strength	
		1 minute after onset	8 minutes after onset
IS inflow (ml/kg/min)	0.14	0.13	0.13
LD outflow (ml/kg/min)	0.14	0.10	0.13
IS pressure (mmHg)	-3.4	-3.3	-3.0

* IS = interstitial space; LD = lymphatic ducts

Right and left ventricular stroke volume decreased and the heart rate increased compared to the physiological situation. Together this led to a decrease in cardiac output. Table 4 presents the pressure changes in the blood containing compartments of the hemodynamics model of Explain, secondary to

PPV, compared to the physiological situation. The pressure in the atria (RA and LA) and ventricles (RV and LV) is increased. The pressure in the arterial system (AA, AAR, AD, and PA) is decreased. The pressure in the extra-thoracic compartments of the capillary system (BR, LS, INT, KID, RLB, RL, and LL) is also decreased, except for the pressure in RUB, which is increased. The pressure in the intrathoracic compartments of the capillary system (COR, RL, and LL) is increased. The pressure in the venous system (IVCE, IVCI, SVC, and PV) is increased.

Table 4: Pressure change in the blood containing components of Explain secondary to PPV compared to the physiological situation.

	LL	PV	LA	LV	AA	AAR	AD
Pressure change compared to physiological situation	↑	↑	↑	↑	↓	↓	↓
	COR	BR	RUB	LS	INT	KID	RLB
	↑	↓	↑	↓	↓	↓	↓
	IVCE	IVCI	SVC	RA	RV	PA	RL
	↑	↑	↑	↑	↑	↓	↑

* PPV = positive pressure ventilation; LL = left lung; PV = pulmonary vein; LA = left atrium; LV = left ventricle; AA = ascending aorta; AAR = aortic arch; AD = descending aorta; COR = coronary arteries; BR = brain; RUB = remainder upper body; LS = liver and spleen; INT = intestines; KID = kidneys; RLB = remainder lower body; IVCE = extra-thoracic inferior vena cava; IVCI = intrathoracic inferior vena cava; SVC = superior vena cava; RA = right atrium; RV = right ventricle; PA = pulmonary artery; RL = right lung.

Figure 18 a-e shows the pressures inside the IS, IL, LT, LD, and SVC. The dotted line in Figure a marks the onset of PPV. It can be seen that pressure inside the LD and SVC increases as a result of PPV. Also, the shape of the pressure curves of the LD and SVC have changed due to PPV. Figures b, c, d, and e show the pressures after 1, 4, 10, and 18 minutes of PPV respectively. It can be seen that the IS, IL, and LT pressures increase over the time course. Mean SVC pressure remains approximately constant. After the instant increase in LD pressure at the onset of PPV, LD pressure slightly decreases until 4 minutes after the start of PPV. Ten minutes after the start of PPV, the pressure in the LD has increased again. After 18 minutes of PPV, the LD pressure has further increased. Thereafter, the mean pressures are approximately constant, and a new steady state is reached. The pressure increase in the LT and LD secondary to intrinsic contraction varies.

As during SV, lymph flow between the IS and IL, and the IL and LT is secondary to extrinsic pumping of the IL. Flow between the LT and LD is mainly a result of respiration. However, during PPV flow occurs at the end of expiration, whereas during SV lymph flow occurs at the end of inspiration. LD outflow is secondary to intrinsic pumping of the LD, as during SV.

IS inflow, LD outflow, and IS pressure during SV and PPV are presented in Table 5. IS inflow slightly decreases as a result of PPV. LD outflow initially decreases and becomes zero. LD outflow eventually resumes and becomes equal to IS inflow. From that moment, 18 minutes after the onset of PPV, a new steady state is reached. IS pressure increases as a result of PPV.

When PPV is switched off and SV is resumed, LD outflow temporarily increases to a maximum of 0.55 ml/kg/min, IS inflow slightly increases to 0.14 ml/kg/min, and IS pressure decreases. Thereafter LD outflow decreases again. After 10 minutes steady state is reached, both IS inflow and LD outflow are 0.14 ml/kg/min, IS pressure is -3.4 mmHg.

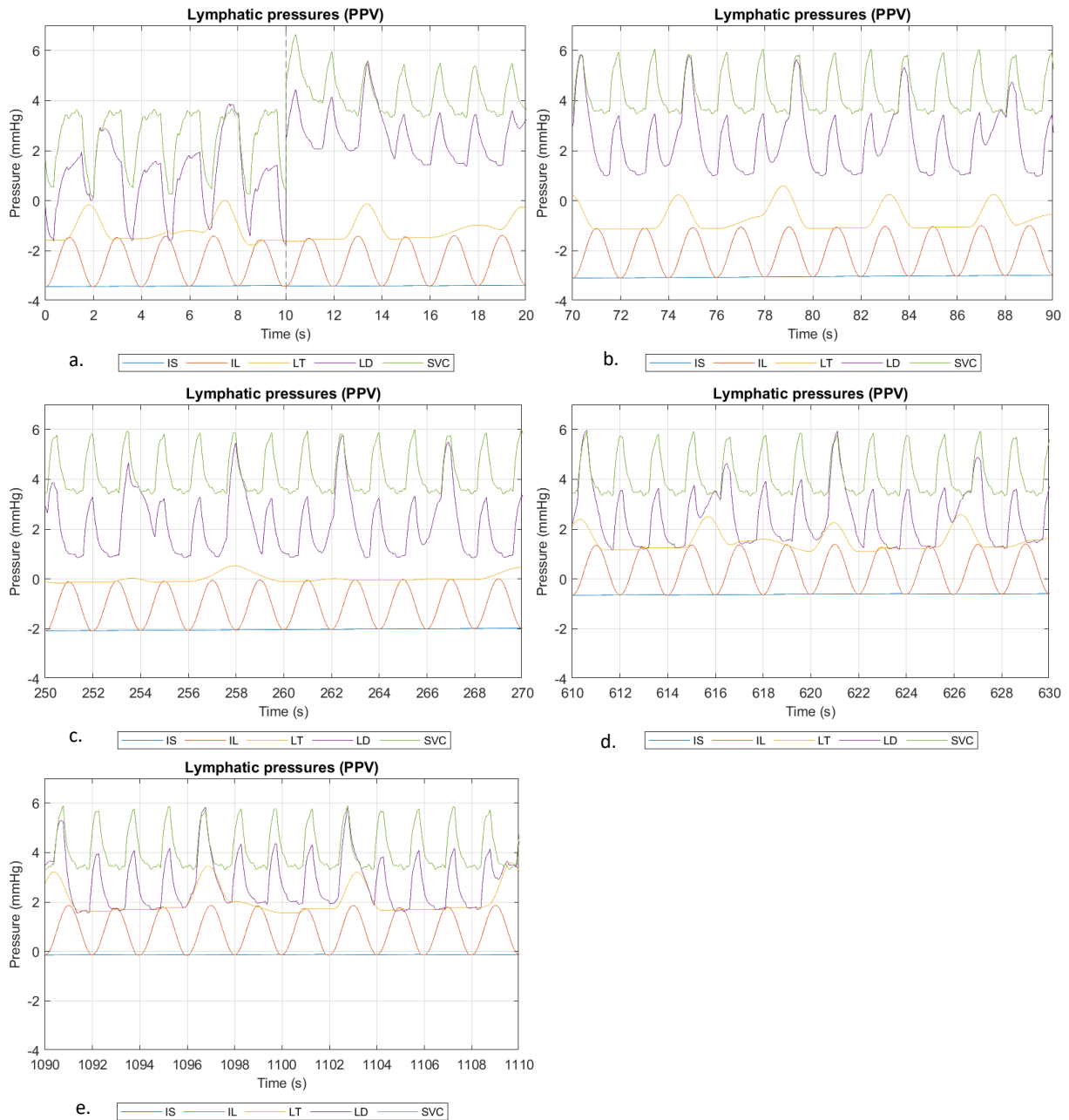


Figure 18: Lymphatic pressures during positive pressure ventilation. The dotted line in figure a. shows the onset of PPV. Figure b-e show the pressures after 1, 4, 10 and 18 minutes of PPV, respectively. IS = interstitial space; IL = initial lymphatics; LT = lymphatic trunks; LD = lymphatic ducts; SVC = superior vena cava.

Table 5: IS inflow, LD outflow and IS pressure under physiological conditions and during PPV.

	Physiological situation	PPV			
		1 minute after onset	4 minutes after onset	10 minutes after onset	18 minutes after onset
IS inflow (ml/kg/min)	0.14	0.14	0.13	0.12	0.12
LD outflow (ml/kg/min)	0.14	0.04	0.0	0.06	0.12
IS pressure (mmHg)	-3.4	-3.1	-2.1	-0.6	-0.1

* PPV = positive pressure ventilation; IS = interstitial space; LD = lymphatic ducts

When using higher ventilator settings (PIP 17.65 mmHg (24 cmH₂O) and PEEP 7.36 mmHg (10 cmH₂O), the other settings were the same as for mild ventilator settings), more fluid accumulates in the IS resulting in an IS pressure of 0.9 mmHg at steady state. IS inflow and LD outflow have decreased to 0.11 ml/kg/min.

The influence of only PIP or PEEP, on interstitial fluid accumulation was investigated. Increasing PIP to 17.65 mmHg (24 cmH₂O) (all other settings were kept the same as for mild ventilator settings) resulted in a new steady state with an IS pressure of 0.0 mmHg, and an IS inflow and LD outflow of 0.12 ml/kg/min. Increasing PEEP to 4.41 mmHg (6 cmH₂O) (all other settings were kept the same as for mild ventilator settings) resulted in a new steady state with an IS pressure of 0.4 mmHg, and an IS inflow and LD outflow of 0.11 ml/kg/min.

Feedback Mechanism

The feedback mechanism model changes intrinsic contraction strength, E_{amp} , and intrinsic contraction frequency, $freq$, based on the controlled variables (cv) flow ($f_{LD, SVC}$) and transmural pressure ($p_{tm, LD}$), to compensate for changes in extrinsic pumping.

The influence of a decreased ventricular contractility and PPV on these controlled variables and thus E_{amp} and $freq$ is presented below.

Figure 19 shows the mean LD outflow and mean LD transmural pressure on the left y-axes, and the intrinsic contraction frequency and maximum increase in elastance during contraction, E_{amp} , on the right y-axes. The length of the left y-axes is $CV_{max} - CV_{min}$. The first 2 minutes shows the behavior under physiological conditions. After 2 minutes, the contraction strength of the ventricles was lowered to 50% of its original value.

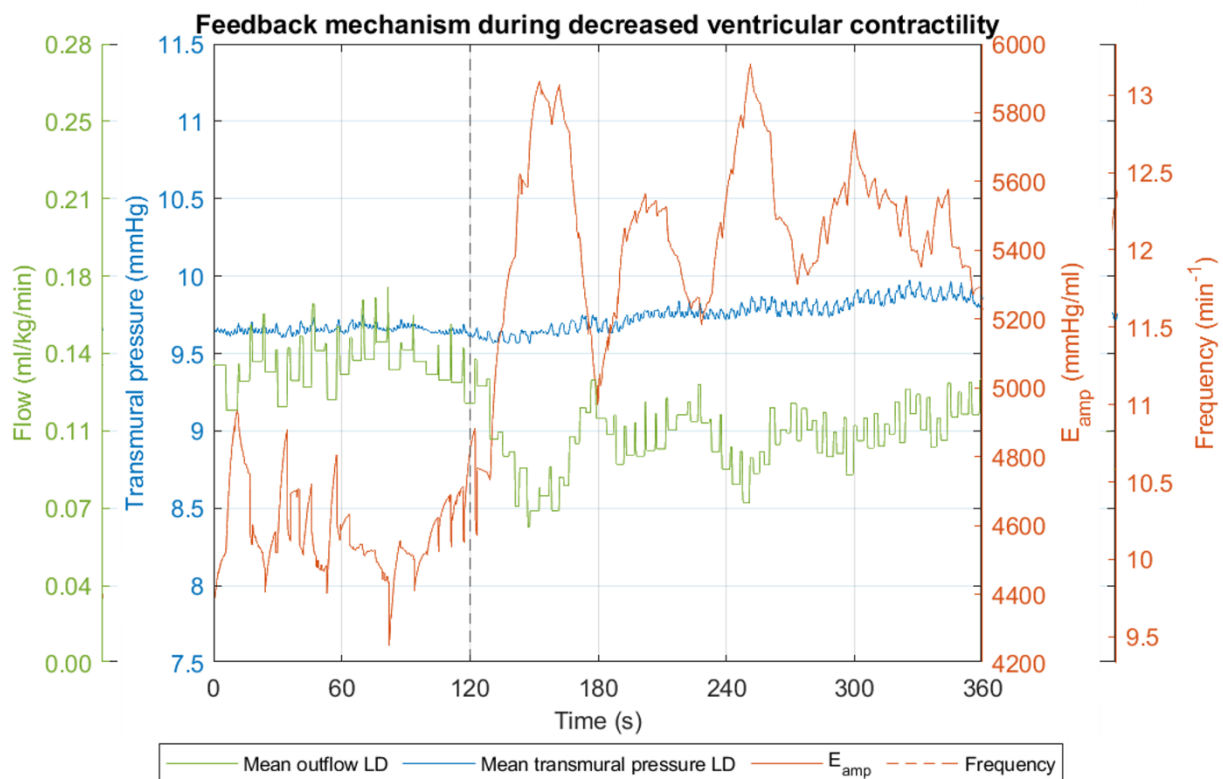


Figure 19: Mean LD outflow and mean LD transmural pressure on the left y-axes, and E_{amp} and contraction frequency of the intrinsic pump on the right y-axes. The dotted line marks the onset of a decreased ventricular contraction strength. LD = lymphatic ducts; E_{amp} = maximum increase in elastance during intrinsic contraction.

During the first 2 minutes, the mean LD transmural pressure curve shows small variations but is relatively constant. Mean LD outflow is calculated over a period of 36 seconds. As the flow is pulsatile with a varying frequency, this results in abrupt changes in mean LD outflow. When the ventricular contraction strength is decreased (dotted line), the mean LD outflow starts to increase after which it decreases, this course repeats itself. The mean LD outflow curve shows a wavy pattern. The amplitude of the waveform decreases over time. Mean LD transmural pressure slightly increases. Intrinsic contraction frequency and E_{amp} increase as the mean LD outflow decreases and vice versa.

A decrease in ventricular contraction strength resulted in an increase in IS pressure to -3.0 mmHg. When the feedback mechanism was disabled, a decrease in ventricular contraction strength resulted in an increase in IS pressure to -2.8 mmHg.

Figure 20 shows the mean LD outflow and mean LD transmural pressure on the left y-axes, and the intrinsic contraction frequency and E_{amp} on the right y-axes. The length of the left y-axes is $CV_{max} - CV_{min}$. The first 2 minutes shows the behavior under physiological conditions (spontaneous ventilation). After 2 minutes, PPV with mild ventilator settings is turned on and SV is switched off.

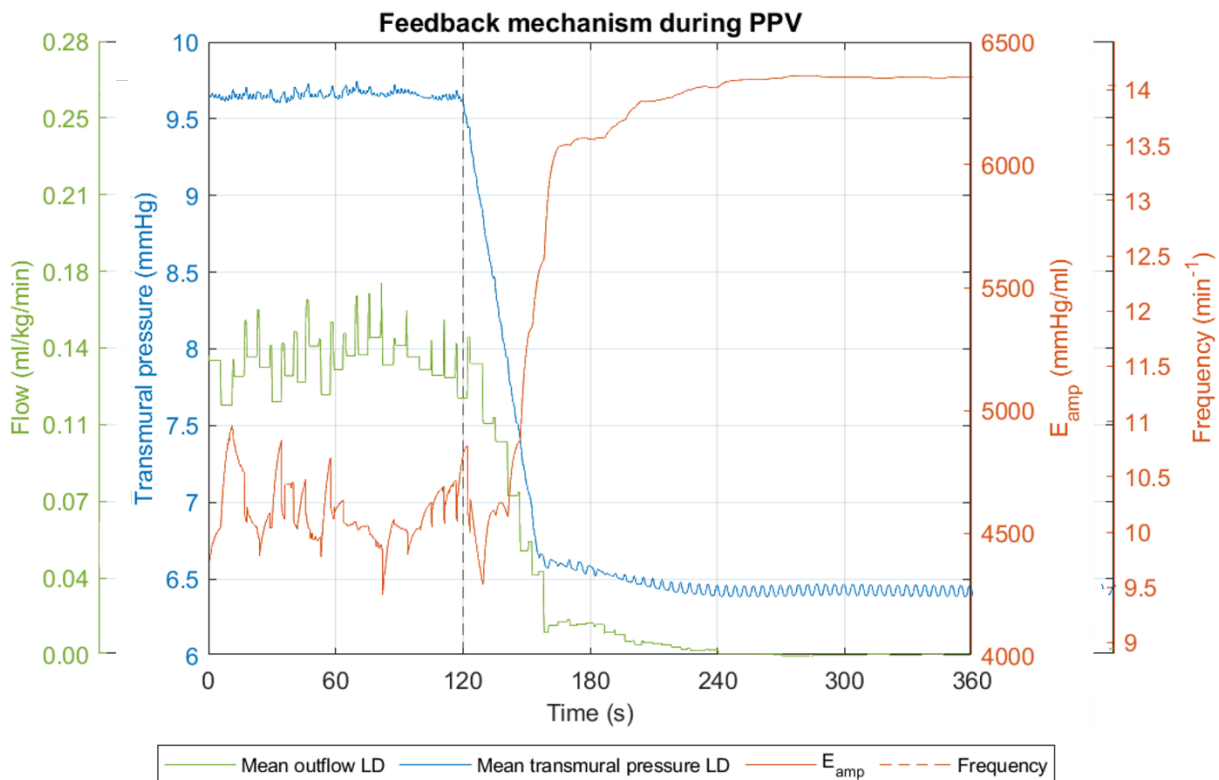


Figure 20: Mean LD outflow and mean LD transmural pressure on the left y-axes, and E_{amp} and contraction frequency on the right y-axes. The dotted line marks the onset of PPV. PPV = positive pressure ventilation; LD = lymphatic ducts; E_{amp} = maximum increase in elastance during intrinsic contraction.

Under physiological conditions, mean LD transmural pressure and mean LD outflow are relatively constant. The abrupt changes in mean LD outflow are again due to the fact that the flow is pulsatile with a varying frequency. From the onset of PPV, mean LD transmural pressure and mean LD outflow decrease fast. Note that LD transmural pressure is the intralymphatic pressure minus the intrathoracic pressure, intrathoracic pressure is positive during PPV instead of negative during SV. After 36 seconds mean LD transmural pressure and outflow keep decreasing but at a slower pace. Contraction frequency and E_{amp} increase after the onset of PPV, after 36 seconds the degree of increase reduces.

PPV resulted in an increase in IS pressure to -0.1 mmHg. When the feedback mechanism was disabled, PPV resulted also in an increase in IS pressure to -0.1 mmHg.

As both LD transmural pressure and LD outflow change over time, it is hard to distinguish the effect of both variables. Therefore, also one simulation is performed in which the intrinsic pumping only depends on LD outflow, shown in Figure 21. And one simulation is performed in which the intrinsic pumping only depends on LD transmural pressure, shown in Figure 22. The first 30 seconds is under physiological conditions, after 30 seconds PPV is switched on and SV is switched off.

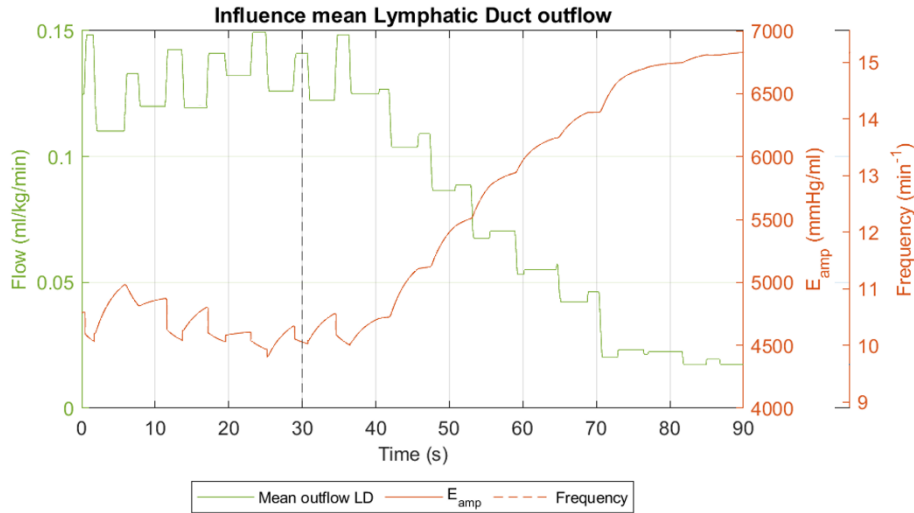


Figure 21: Mean LD outflow, E_{amp} and contraction frequency. Here intrinsic pump function only depends on LD outflow.

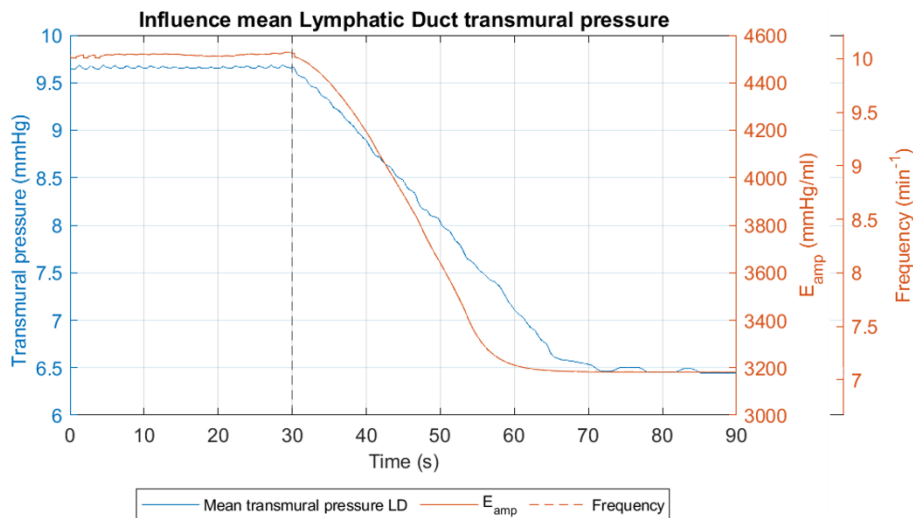


Figure 22: Mean LD pressure, E_{amp} and contraction frequency. Here intrinsic pump function only depends on LD pressure.

In Figure 21 it can be seen that contraction frequency and E_{amp} increase as the mean LD outflow decreases, which is in accordance with Equation 19, whereby the last term on the right side of the equation is equal to zero. In Figure 22 it can be seen that contraction frequency and E_{amp} decrease as the mean LD transmural pressure decreases, which is in accordance with Equation 19, whereby the second term on the right side of the equation is equal to zero. From approximately one minute, contraction frequency and E_{amp} do not further decrease even though the LD transmural pressure keeps increasing.

Discussion

5.1 Interpretation of the Results

In this study, a mathematical model of the neonatal lymphatic transport system that interacts with the hemodynamics and ventilatory model of Explain is developed. Parameters were chosen to obtain target values for the IS pressure and flow through the LD under physiological conditions. Two situations, namely a decreased ventricular contraction strength (heart failure) and PPV, are simulated and compared to the literature for validation of the model.

Physiological Situation

The extrinsic pump pressure acting on the IL is modeled such that it results in lymph flow from the IS to the IL and from the IL to the LT. Flow from the IS to the IL is secondary to a decrease in IL pressure. However, in real life, flow from the IS to the IL is secondary to an increase in IS pressure, as is described in section 2.1. Flow from the IL to the LT is secondary to an increase in IL pressure due to extrinsic pumping, as is described in the literature.

The simulations show that under physiological conditions, flow from the (extra-thoracic) LT to the (intrathoracic) LD is secondary to inspiration. This corresponds to what is described in the literature. It is described that a decrease in intrathoracic pressure during inspiration provides a favorable gradient for intrathoracic thoracic duct filling^{32,48}.

The literature presents various findings regarding the influence of respiration on thoracic duct outflow²⁵. Some studies have demonstrated lymph flow across the LVJ during inspiration, while others concluded that lymph flow across the LVJ was continuous but largest during expiration. Additionally, there are studies suggesting that lymphatic duct outflow occurs independently of the respiratory cycle. Kelly et al. propose that thoracic duct contractions are an important factor in securing the successful return of lymph to the venous system³². In our model lymphatic duct outflow is primarily driven by LD contractions and is independent of respiration. The latter can be explained. Respiration alters intrathoracic pressure, affecting all intrathoracic structures, including both the LD and the SVC. Consequently, the pressure gradient between these structures remains constant, ensuring that LD outflow is unaffected. However, if respiration induces a larger pressure change in one of these compartments, it will consequently affect LD outflow.

In most lymphatic vessels, intrinsic pumping is essential for lymph propulsion⁴⁹. However, in our model, extrinsic pumping is generally sufficient to propel lymph to the next compartment, except for the propulsion of lymph from the LD to the SVC. This is likely due to the limited number of contracting compartments in the model. In reality, lymphatic vessels comprise numerous lymphangions, which are contracting compartments, whereas the model represents lymphatic vessels with only one contracting compartment. If the LT were represented by multiple contracting compartments, the pressure decrease in the LD due to inspiration would only result in lymph flow from the distal part of the LT to the LD. When the volume decrease in the distal part of the LT is significant enough to cause the pressure to drop below that of the preceding compartment, it also facilitates lymph flow into the distal part of the LT from the preceding compartment. However, the extent of this effect will be limited. Therefore, in the absence of sufficient extrinsic pumping, lymph propulsion through the proximal part of the LT, which consists of multiple contracting elements, would rely on the intrinsic contractions of the LT.

Szabo and Magyar performed pressure measurements during the cannulation of dogs⁵⁰. They found a mean intralymphatic pressure in the thoracic duct of 5.11 mmHg, whereas the pressure in the jugular vein was 5.83 mmHg. In more peripheral lymphatic vessels the pressures were lower, for instance, the pressure in the intestinal trunk was 3.60 mmHg and the pressure in the femoral lymph vessels was 0.51 mmHg. When comparing these pressures to the pressure in the LD, SVC, LT, and IL respectively, the pressures in the model are lower. However, both the experimental data and the model show an

increase in pressure from the peripheral lymphatics towards the central lymphatics. Additionally, achieving specific pressures in the IL, LT, and LD was not the primary objective.

The simulations show that lymph flow is pulsatile, as modeled, which corresponds to what is described in the literature⁴⁸.

Elevated Central Venous Pressure

The simulations demonstrate that a decrease in ventricular contraction strength results in a reduced left and right ventricular stroke volume. Therefore, less blood is pumped into the arterial system which results in a decrease in arterial and capillary pressures. Moreover, as less blood is pumped away by the ventricles, blood accumulates in front of the ventricles, increasing venous pressure.

Lu et al. investigated the effect of elevated CVP, induced by tricuspid regurgitation (TR), on thoracic duct flow in animals⁵¹. Thoracic duct flow and pressure were measured two weeks before TR surgery (baseline) and on days 1, 2, 3, 7, 14, and 28 after TR surgery. They observed that the thoracic duct flow doubled nearly immediately following induction of TR and reached a plateau at approximately 10-fold that of baseline by two days. The pressure in the thoracic duct increased proportionally to the elevated CVP. Lu et al. state that an elevated CVP in congestive heart failure increases lymph production due to an increase in transcapillary filtration from the capillary bed into the interstitial space, and impedes thoracic duct flow by increasing the thoracic duct afterload pressure at the LVJ. As TR resulted in a sustained increase in lymphatic duct flow, Lu et al. concluded that increased lymph production is dominant over increased thoracic duct afterload. During the 4 weeks of study duration, they did not observe tissue edema or effusions. They hypothesized that this was because the right heart was still in a compensated state.

In our model, decreased ventricular contraction strength, indicative of heart failure, results in an elevated SVC pressure, indicative of CVP. Therefore, impeding LD outflow and causing a reduction in LD outflow. As IS inflow remains approximately constant, this results in fluid accumulation in the lymphatic system, however only minimal. IS pressure increases, resulting in a decrease in IS inflow. LD pressure increases proportionally with SVC pressure, corresponding to the findings of Lu et al. This pressure increase restores LD outflow. A new steady state is reached when IS inflow and LD outflow are equal. In this steady state, IS inflow and LD outflow are slightly lower compared to the physiological situation. These observations are not consistent with the findings of Lu et al., they describe an increase in thoracic duct flow secondary to an elevated CVP in heart failure. In our model, LD outflow did not increase secondary to a decreased ventricular contraction strength because IS inflow, i.e. transcapillary filtration, did not increase.

An increase in transcapillary filtration due to an elevated CVP might be explained as follows. As described in section 2.2, transcapillary filtration depends on the hydrostatic and osmotic pressure gradient between the capillaries and the interstitial space. The net pressure gradient may also favor the reabsorption of interstitial fluid back into the capillaries. Transcapillary filtration and reabsorption occur across the entire extent of the capillary bed, from the arteriolar end of the capillaries to the venule end of the capillaries. The hydrostatic and osmotic pressure in the interstitial space is approximately the same near the arteriolar and venule end of the capillaries. Capillary osmotic pressure is also approximately constant along the entire capillary bed. Capillary hydrostatic pressure is lower at the venule end compared to the arteriolar end. Normally, at the arteriolar end of the capillaries, the hydrostatic pressure gradient outweighs the osmotic pressure gradient, resulting in filtration. At the venule end of the capillaries, the osmotic pressure gradient outweighs the hydrostatic pressure gradient, resulting in reabsorption. Across the total capillary bed, there is a net production of interstitial fluid. Increased CVP raises venule hydrostatic pressure, reducing the difference between the

hydrostatic and osmotic pressure gradient. This results in a decrease in reabsorption, and thus an increase in the net interstitial fluid production across the total capillary bed.

In our model, there is only one compartment that represents the entire vasculature of an organ or tissue. This compartment is connected to the IS. This compartment's hydrostatic pressure resembles the hydrostatic pressure at the arteriolar end of the capillaries, resulting in interstitial fluid production. There is no reabsorption of interstitial fluid as the IS is not connected to a compartment of which the hydrostatic pressure represents that of the venule end of the capillary network.

It is expected that if flow between a blood-containing compartment and the IS depends on the osmotic and hydrostatic pressure resembling the pressures at the arteriolar and venule end of the capillary bed, an elevated CVP will result in an increase in interstitial fluid production in the model.

The total interstitial fluid production across the capillary bed is the sum of the flow at the arteriolar and venule end. To implement this in the model, Equation 9 can be adjusted to account for both arterial and venous pressures:

$$f_{i,k}(t) = L_p S [p_i(t) + p_j(t) - 2[p_k(t) + \sigma \Delta \pi]]. \quad (28)$$

$f_{i,k}$ is the flow between blood capacitance i from the hemodynamics model, and lymph capacitance k from the lymphatics model. L_p is the hydraulic conductivity in $\text{cm}/\text{min} \cdot \text{mmHg}$, S is the capillary surface area in cm^2 , and σ is the osmotic reflection coefficient which is dimensionless. p_i is the hydrostatic pressure in blood capacitance i , p_j is the hydrostatic pressure in the consecutive blood capacitance, both in mmHg . p_k is the hydrostatic pressure in lymph capacitance k , also in mmHg . $\Delta \pi$ is the osmotic pressure differences between blood capacitance i and lymph capacitance k in mmHg . The osmotic pressure in blood capacitance i and j is equal.

The degree of fluid accumulation in the lymphatic system depends on the elastance of the lymphatic components, while the time to reach a new steady state depends on the resistance between components. Parameter values were chosen to achieve target IS pressure and LD outflow under physiological conditions, making the exact degree of fluid accumulation and time to reach a new steady state after the induction of a decreased ventricular contraction strength less relevant as long as the direction of change is correct.

Positive Pressure Ventilation

The simulations show that PPV increases the pressure in the intrathoracic blood-containing compartments, except for the PV. Both right and left ventricular stroke volume decrease secondary to PPV, as is described in the literature⁵². The decrease in right ventricular stroke volume is attributed to a reduced venous return (decreased preload) and increased pulmonary vascular resistance (increased afterload), both resulting from elevated intrathoracic pressure. Consequently, left ventricular preload decreases, leading to a reduced left ventricular stroke volume. This reduction in ventricular stroke volumes results in decreased arterial pressures, which is consistent with our simulations. Blood accumulates in the extra-thoracic venous system, increasing the pressure in these compartments.

The simulations also show that PPV results in fluid accumulation in the lymphatic system until a new steady state is reached. In this new steady state, LD outflow is slightly lower compared to the physiological situation. Unlike the case with decreased ventricular contraction strength, during PPV, fluid initially accumulates in the extra-thoracic lymphatic compartments before affecting the intrathoracic compartments. The extent of fluid accumulation in the lymphatic system is larger due to the larger pressure increase in the SVC due to PPV compared to a decreased ventricular contraction strength.

Animal studies have demonstrated that lymphatic production increases due to PPV⁴⁸. However, our model did not show an increase in lymph production under PPV. Instead, simulations indicated slightly reduced lymph production due to increased IS pressure. This discrepancy can be explained similarly to the decreased lymph production observed with reduced ventricular contraction strength.

Khan et al. investigated the effect of PPV on lymphatic flow in pediatric patients, assessing thoracic duct outflow by measuring contrast clearance in patients with lymphatic failure⁴⁸. At baseline PPV settings, poor antegrade flow through the thoracic duct, pooling of lymph in the neck, congestion in the retroperitoneum, and retrograde flow through multiple cutaneous channels were observed. Removal of positive pressure led to a decrease in thoracic duct pressure and CVP, resulting in improvement of thoracic duct flow with decreased contrast clearance time.

In our simulations, the removal of the positive pressure also increased LD outflow, consistent with observations of Khan et al. Initially, LD outflow increases before stabilizing at a new steady state. In this new steady state, LD outflow is slightly higher compared to during PPV. Khan et al. did not report the long-term effects of PPV removal on thoracic duct flow.

It is important to distinguish between the initial and long-term effects of (removal of) PPV on lymph drainage. Initially, lymphatic duct flow decreases secondary to PPV as the influx of lymph into the intrathoracic thoracic duct decreases and eventually stops. Lymph accumulates in the extra-thoracic lymphatic system, restoring lymphatic flow between the extra- and intrathoracic lymphatic vessels. This results in fluid accumulation in the intrathoracic lymphatic. As intrathoracic lymphatic pressure increases, lymphatic duct flow gradually improves until it matches lymphatic production. CVP is increased secondary to PPV, and thus lymphatic production is increased. Therefore, in the long term, lymphatic duct flow also increases secondary to PPV.

The simulations indicate that increasing PIP or PEEP leads to more fluid accumulation by raising intrathoracic pressure. Increasing PEEP has a larger effect on fluid accumulation than increasing PIP, as increasing PEEP results in a consistently higher pressure, whereas PIP only raises peak pressures.

Again, the exact degree of fluid accumulation and time to reach a new steady state after the onset of PPV is less relevant as long as the direction of change is correct.

Feedback Mechanism

The simulations show that after the initiation of a decreased ventricular contractility, the LD outflow exhibits a wavy pattern. This wavy pattern diminishes over time. The LD transmural slightly increases after the initiation of a decreased ventricular contractility. E_{amp} and contraction frequency, also show a wavy pattern, inverse to that of LD outflow.

Given the constant resistance between the LD and SVC, and the unchanged mean SVC pressure and intrathoracic pressure, it can be concluded that variations in intrinsic pump contraction strength and/or frequency influence LD outflow.

Initially, LD outflow decreases due to a reduced ventricular contraction strength. Subsequently, as intrinsic pump contraction strength and frequency increase, LD outflow rises. This increase in outflow, in turn, decreases intrinsic pump contraction strength and frequency, resulting in the observed wavy and inverse patterns in the LD outflow curve and the curve of E_{amp} and contraction frequency.

The feedback mechanism limits the increase in IS pressure secondary to a decreased ventricular contraction strength compared to the situation without feedback. However, the feedback mechanism is not able to entirely prevent fluid accumulation. Despite the increased contraction frequency and

strength relative to the physiological situation, LD outflow remains lower than IS inflow, leading to fluid accumulating in the lymphatic system.

The difference in pressure increase between the feedback and no feedback scenarios is due to the sustained increase in contraction strength and frequency resulting from the elevated LD transmural pressure. Nonetheless, the effect of LD outflow on contraction strength and frequency is not sufficient. The contraction strength and frequency required for sufficient LD outflow are not maintained because the induced increase in LD outflow subsequently causes a reduction in contraction frequency and strength.

The simulations also show that upon initiating PPV, LD outflow and LD transmural pressure decrease. A reduction in LD outflow triggers an increase in intrinsic pump contraction frequency and strength, while a decrease in LD transmural pressure results in a decrease in intrinsic pump contraction frequency and strength, as modeled. A decrease in both LD outflow and LD transmural pressure resulted in an increase in contraction frequency and strength. Despite the increase in contraction strength and frequency, LD outflow does not rise, rendering these contractions inefficient. Consequently, there is no difference in IS pressure increase comparing feedback and no feedback scenarios.

This inefficiency can be explained as follows. Intrinsic contractions elevate intralymphatic pressure through muscle cell contraction in the lymphatic vessel wall. In our model, intrinsic contractions are simulated by increased elastance. However, pressure also depends on volume. Therefore, an increase in elastance does not always translate to increased pressure.

Both LD and SVC pressure increase secondary to PPV, halting flow between the LT and the LD. Initially, there is still flow between the LD and SVC, but as lymph flow into the LD ceases, the LD volume decreases. Subsequently, LD outflow decreases despite increased intrinsic pump contraction strength and frequency.

PPV also enhances intrinsic pump contraction strength and frequency of the LT. Lymph accumulates in the LT as there is no outflow. Initially, LT volume is below its unstressed volume, so fluid accumulation reduces the difference between volume and unstressed volume. Therefore, the pressure difference between the LT and LD is not overcome by an increased intrinsic pump contraction strength.

PPV immediately reduces both LD transmural pressure and LD outflow. However, the feedback mechanism uses the mean transmural pressure and mean flow over 36 seconds as input. These mean values gradually decrease, resulting in a gradual increase in E_{amp} and contraction frequency.

5.2 Strengths and Limitations

This study aimed to model lymph formation by transcapillary filtration, and lymph propulsion through the lymphatic vessel network and drainage into the central venous circulation via intrinsic and extrinsic pumping. The model comprises a limited number of components and the equations have deliberately been kept as simple as possible. Several assumptions were made.

First, it was assumed that the valves provide constant resistance to antegrade flow and prevent retrograde flow. This simplified representation was chosen to limit the number of parameters that had to be estimated. Microvalves and intraluminal valves are modeled similarly, despite their functional differences. Intraluminal valves can be more realistically modeled with a resistance varying with transvalvular pressure according to a sigmoidal function, as done by Bertram et al.⁹ The resistance is maximal when the valve is closed and decreases as the valve opens with increasing transvalvular pressures. Primary valves can be modeled more realistically by a nonlinear function depending on transmural pressure, as described by Ikhimwin et al.¹⁰ Implementing these functions would make the model more realistic, though it is expected that they would not significantly influence the mean lymphatic flow rate.

Second, the compliance of the interstitial space is assumed to be constant. In reality, the interstitial space exhibits a variable compliance²². Fluid added to the interstitial space in its low-compliance range significantly raises interstitial pressure, driving fluid into the lymphatic system. In this range, lymphatic drainage matches interstitial fluid production, maintaining a stable interstitial volume. If the interstitial space is already expanded and in its high-compliance range, added fluid raises the interstitial pressure only moderately.

Third, it is assumed that an increase in transmural pressure results in an increase in intrinsic contraction strength. However, experimental data from Gashev et al. showed that contraction strength initially increases with rising transmural pressure until a maximum value, after which further increases in transmural pressure lead to a decrease in contraction strength³⁷. The latter was not modeled.

Many models for parts of the lymphatic system have been described in the literature. The main advantage of our model is that it represents the entire lymphatic transport system and is integrated with models of the circulatory and respiratory systems. This integration allows for the investigation of interactions between these systems.

5.3 Future Research

Multiple adaptations should be made to improve the model. As previously mentioned, transcapillary filtration should depend on hydrostatic and osmotic pressures at both the arteriolar and venule ends of the capillary bed, rather than just the arteriolar end. Additionally, intrinsic contractions should be modeled as an external pressure acting on the lymphatic vessels instead of a change in elastance. Future research should focus on improving the feedback mechanism model and expanding the lymphatics model by dividing the interstitial space into separate compartments for different organs and tissues.

Feedback to the intrinsic pump is essential for regulating lymphatic flow. As previously described, contraction strength and frequency depend on multiple factors. The current model incorporates the influence of transmural pressure and lymph flow as a linear dependency independent of time. Gashev et al. performed experiments on rat mesenteric lymphatics and found that upon the imposition of flow, the contraction frequency is rapidly inhibited, then slowly returns to baseline values, while contraction strength gradually decreases⁵³. These time-dependent changes are not incorporated into the model. Additionally, more realistic values for E_{amp} and frequency should be determined, and the ratio between E_{amp} and frequency should be optimized.

In the model, there is a single compartment representing the entire interstitial space. Dividing this into separate compartments for different organs would allow for the modeling and investigation of more specific pathological conditions. The first step would be to create distinct interstitial compartments for extra-thoracic and intrathoracic structures. For example, PPV increases intrathoracic pressure, temporarily halting lymph propulsion from extra-thoracic to intrathoracic compartments and causing lymph accumulation in extra-thoracic tissues. As PPV increases the pressure in both the LD and SVC, lymph drainage of intrathoracic tissues is not halted, and lymph will not accumulate in these structures. Furthermore, interstitial fluid production varies significantly between organs, and different symptoms occur depending on the location of edema and effusions.

Implementing these adaptations will make the model more realistic and improve its utility in understanding lymphatic system interactions and pathophysiology.

5. Conclusion

A preliminary model of the neonatal lymphatic transport system, which interacts with the circulatory and respiratory systems, has been developed. Initial simulations under pathological conditions did not fully align with in vivo measurements in animals. To address these discrepancies, minor adjustments to the model are proposed. Our modeling effort has provided new insights into the (patho)physiology of the lymphatic system and enhanced our understanding of its interactions with other systems.

References

1. Ozdowski L, Gupta V. *Physiology, Lymphatic System.*; 2023.
2. Mehrara BJ, Radtke AJ, Randolph GJ, et al. The emerging importance of lymphatics in health and disease: an NIH workshop report. *Journal of Clinical Investigation*. 2023;133(17). doi:10.1172/JCI171582
3. Bengtsson BOS, van Houten JP. Central edema in critically ill neonates. *Case Reports in Perinatal Medicine*. 2019;8(2). doi:10.1515/crpm-2019-0037
4. Shih YT, Su PH, Chen JY, Lee IC, Hu JM, Chang HP. Common Etiologies of Neonatal Pleural Effusion. *Pediatr Neonatol*. 2011;52(5):251-255. doi:10.1016/j.pedneo.2011.06.002
5. Zani-Ruttenstock E, Zani A. Neonatal Ascites. In: *Pediatric Surgery*. Springer Berlin Heidelberg; 2017:1-8. doi:10.1007/978-3-642-38482-0_73-1
6. Ramirez-Suarez KI, Tierradentro-Garcia LO, Smith CL, et al. Dynamic contrast-enhanced magnetic resonance lymphangiography. *Pediatr Radiol*. 2022;52(2):285-294. doi:10.1007/s00247-021-05051-6
7. Bertram CD, Macaskill C, Moore JE. Simulation of a Chain of Collapsible Contracting Lymphangions With Progressive Valve Closure. *J Biomech Eng*. 2011;133(1). doi:10.1115/1.4002799
8. Bertram CD, Macaskill C, Davis MJ, Moore JE. Development of a model of a multi-lymphangion lymphatic vessel incorporating realistic and measured parameter values. *Biomech Model Mechanobiol*. 2014;13(2):401-416. doi:10.1007/s10237-013-0505-0
9. Bertram CD, Macaskill C, Davis MJ, Moore JE. Valve-related modes of pump failure in collecting lymphatics: numerical and experimental investigation. *Biomech Model Mechanobiol*. 2017;16(6):1987-2003. doi:10.1007/s10237-017-0933-3
10. Ikhimwin BO, Bertram CD, Jamalain S, Macaskill C. A computational model of a network of initial lymphatics and pre-collectors with permeable interstitium. *Biomech Model Mechanobiol*. 2020;19(2):661-676. doi:10.1007/s10237-019-01238-x
11. Bertram CD. Modelling secondary lymphatic valves with a flexible vessel wall: how geometry and material properties combine to provide function. *Biomech Model Mechanobiol*. 2020;19(6):2081-2098. doi:10.1007/s10237-020-01325-4
12. Xie PY, Morris CJ, Bertram C, Zaweija D, James E. Moore J. Modeling Mechanical Feedback Mechanisms in a Multiscale Sliding Filament Model of Lymphatic Muscle Pumping. *bioRxiv*. Published online January 1, 2022:2022.11.30.518078. doi:10.1101/2022.11.30.518078
13. Antonius TAJ, van Meurs WL, Westerhof BE, de Boode WP. An Integrated Model for Simulation of Neonatal Physiology, Part I: The Cardiovascular System [Paper in preparation].
14. Antonius T. Explain. <https://github.com/Dobutamine/explain-web/tree/main/src/explain>
15. Null M, Arbor TC, Agarwal M. *Anatomy, Lymphatic System.*; 2023.
16. Stewart RH. A Modern View of the Interstitial Space in Health and Disease. *Front Vet Sci*. 2020;7. doi:10.3389/fvets.2020.609583

17. Oliver G, Kipnis J, Randolph GJ, Harvey NL. The Lymphatic Vasculature in the 21st Century: Novel Functional Roles in Homeostasis and Disease. *Cell*. 2020;182(2):270-296. doi:10.1016/j.cell.2020.06.039
18. Moore JE, Bertram CD. Lymphatic System Flows. *Annu Rev Fluid Mech*. 2018;50(1):459-482. doi:10.1146/annurev-fluid-122316-045259
19. Zhang F, Zarkada G, Yi S, Eichmann A. Lymphatic Endothelial Cell Junctions: Molecular Regulation in Physiology and Diseases. *Front Physiol*. 2020;11. doi:10.3389/fphys.2020.00509
20. Chen H, Griffin C, Xia L, Srinivasan RS. Molecular and cellular mechanisms of lymphatic vascular maturation. *Microvasc Res*. 2014;96:16-22. doi:10.1016/j.mvr.2014.06.002
21. Scallan J, Huxley VH, Korthuis RJ. Capillary Fluid Exchange: Regulation, Functions, and Pathology. *Colloquium Series on Integrated Systems Physiology: From Molecule to Function*. 2010;2(1):1-94. doi:10.4199/C00006ED1V01Y201002ISP003
22. Boron WF, Boulpaep EL. *Medical Physiology*. 2nd ed. (O'Grady E, Hall A, eds.). Saunders Elsevier; 2012.
23. Willard-Mack CL. Normal Structure, Function, and Histology of Lymph Nodes. *Toxicol Pathol*. 2006;34(5):409-424. doi:10.1080/01926230600867727
24. Ager A, May MJ. Understanding high endothelial venules: Lessons for cancer immunology. *Oncoimmunology*. 2015;4(6):e1008791. doi:10.1080/2162402X.2015.1008791
25. O'Hagan LA, Windsor JA, Itkin M, Russell PS, Phillips ARJ, Mirjalili SA. The Lymphovenous Junction of the Thoracic Duct: A Systematic Review of its Structural and Functional Anatomy. *Lymphat Res Biol*. 2021;19(3):215-222. doi:10.1089/lrb.2020.0010
26. Pstras L, Waniewski J, Lindholm B. Transcapillary transport of water, small solutes and proteins during hemodialysis. *Sci Rep*. 2020;10(1):18736. doi:10.1038/s41598-020-75687-1
27. Feher J. The Microcirculation and Solute Exchange. In: *Quantitative Human Physiology*. Elsevier; 2012:578-588. doi:10.1016/B978-0-12-800883-6.00055-0
28. Levenbrown Y, Costarino AT. Edema. In: *Nephrology and Fluid/Electrolyte Physiology: Neonatology Questions and Controversies*. Elsevier; 2012:267-284. doi:10.1016/B978-1-4377-2658-9.00016-9
29. Aukland K, Reed RK. Interstitial-lymphatic mechanisms in the control of extracellular fluid volume. *Physiol Rev*. 1993;73(1):1-78. doi:10.1152/physrev.1993.73.1.1
30. Yuan S, Rigor R. Structure and function of exchange microvessels. In: *Regulation of Endothelial Barrier Function*. ; 2010.
31. Jamalian S, Jafarnejad M, Zawieja SD, et al. Demonstration and Analysis of the Suction Effect for Pumping Lymph from Tissue Beds at Subatmospheric Pressure. *Sci Rep*. 2017;7(1):12080. doi:10.1038/s41598-017-11599-x
32. Kelly B, Smith CL, Saravanan M, Dori Y, Hjortdal VE. Spontaneous contractions of the human thoracic duct—Important for securing lymphatic return during positive pressure ventilation? *Physiol Rep*. 2022;10(10). doi:10.14814/phy2.15258

33. Scallan JP, Zawieja SD, Castorena-Gonzalez JA, Davis MJ. Lymphatic pumping: mechanics, mechanisms and malfunction. *J Physiol*. 2016;594(20):5749-5768. doi:10.1113/JP272088
34. Solari E, Marcozzi C, Negrini D, Moriondo A. Lymphatic Vessels and Their Surroundings: How Local Physical Factors Affect Lymph Flow. *Biology (Basel)*. 2020;9(12):463. doi:10.3390/biology9120463
35. Davis MJ, Zawieja SD. Pacemaking in the lymphatic system. *J Physiol*. Published online March 23, 2024. doi:10.1113/JP284752
36. Margaris KN, Black RA. Modelling the lymphatic system: challenges and opportunities. *J R Soc Interface*. 2012;9(69):601-612. doi:10.1098/rsif.2011.0751
37. Gashev AA. Lymphatic Vessels: Pressure- and Flow-dependent Regulatory Reactions. *Ann N Y Acad Sci*. 2008;1131(1):100-109. doi:10.1196/annals.1413.009
38. Santambrogio L. The Lymphatic Fluid. In: ; 2018:111-133. doi:10.1016/bs.ircmb.2017.12.002
39. Swartz M. The physiology of the lymphatic system. *Adv Drug Deliv Rev*. 2001;50(1-2):3-20. doi:10.1016/S0169-409X(01)00150-8
40. Sawdon M, Kirkman E. Capillary dynamics and the interstitial fluid–lymphatic system. *Anaesthesia & Intensive Care Medicine*. 2020;21(7):356-362. doi:10.1016/j.mpaic.2020.04.006
41. Lent-Schochet D, Jialal I. *Physiology, Edema.*; 2024.
42. Wesseling K, Settels J. *Baromodulation Explains Short-Term Blood Pressure Variability*. Plenum Press; 1985.
43. van Meurs W. *Modeling and Simulation in Biomedical Engineering: Application to Cardiorespiratory Physiology*. McGraw-Hill ; 2011.
44. Bertram CD, Macaskill C, Moore JE. Pump function curve shape for a model lymphatic vessel. *Med Eng Phys*. 2016;38(7):656-663. doi:10.1016/j.medengphy.2016.04.009
45. Ilahi M, St Lucia K, Ilahi TB. *Anatomy, Thorax, Thoracic Duct.*; 2023.
46. Kim CR, Katheria AC, Mercer JS, Stonestreet BS. Fluid Distribution in the Fetus and Neonate. In: *Fetal and Neonatal Physiology*. Elsevier; 2017:1081-1089.e3. doi:10.1016/B978-0-323-35214-7.00112-8
47. Leeds SE, Uhley HN, Basch CM, Rosenbaum EH, Yoffey JM. Comparative Studies of Lymph and Lymphocytes of the Thoracic Duct and Right Lymphatic Duct I. Normal Dogs. *Lymphology*. 1971;4:53-57.
48. Khan S, Smith CL, Pinto EM, et al. Effect of positive pressure ventilation on lymphatic flow in pediatric patients. *Journal of Perinatology*. 2023;43(8):1079-1081. doi:10.1038/s41372-022-01563-7
49. Zawieja DC. Contractile Physiology of Lymphatics. *Lymphat Res Biol*. 2009;7(2):87-96. doi:10.1089/lrb.2009.0007
50. Szabó G, Magyar Z. Pressure measurements in various parts of the lymphatic system. *Acta Med Acad Sci Hung*. 1967;23(3):237-241.

51. Lu X, Wang M, Han L, et al. Changes of thoracic duct flow and morphology in an animal model of elevated central venous pressure. *Front Physiol.* 2022;13. doi:10.3389/fphys.2022.798284
52. Corp A, Thomas C, Adlam M. The cardiovascular effects of positive pressure ventilation. *BJA Educ.* 2021;21(6):202-209. doi:10.1016/j.bjae.2021.01.002
53. Gashev AA, Davis MJ, Zawieja DC. Inhibition of the active lymph pump by flow in rat mesenteric lymphatics and thoracic duct. *J Physiol.* 2002;540(3):1023-1037. doi:10.1113/jphysiol.2001.016642
54. Overview of the lymphatic system. <https://www.msmanuals.com/home/quick-facts-heart-and-blood-vessel-disorders/lymphatic-disorders/overview-of-the-lymphatic-system>.
55. Baluk P, McDonald DM. Buttons and Zippers: Endothelial Junctions in Lymphatic Vessels. *Cold Spring Harb Perspect Med.* Published online May 9, 2022:a041178. doi:10.1101/cshperspect.a041178
56. Shou Y, Johnson SC, Quek YJ, Li X, Tay A. Integrative lymph node-mimicking models created with biomaterials and computational tools to study the immune system. *Mater Today Bio.* 2022;14:100269. doi:10.1016/j.mtbio.2022.100269
57. Anatomical location of lymphatic trunks and ducts in the thorax. *McGraw-Hill Companies, Inc.* Accessed July 30, 2024. <https://pdfs.semanticscholar.org/7e74/0e9a912b1ac7145cae2dc03cce7595379274.pdf>

Appendix A

Hydraulic circuit representation of the hemodynamics model of Explain from Antonius et al.¹³

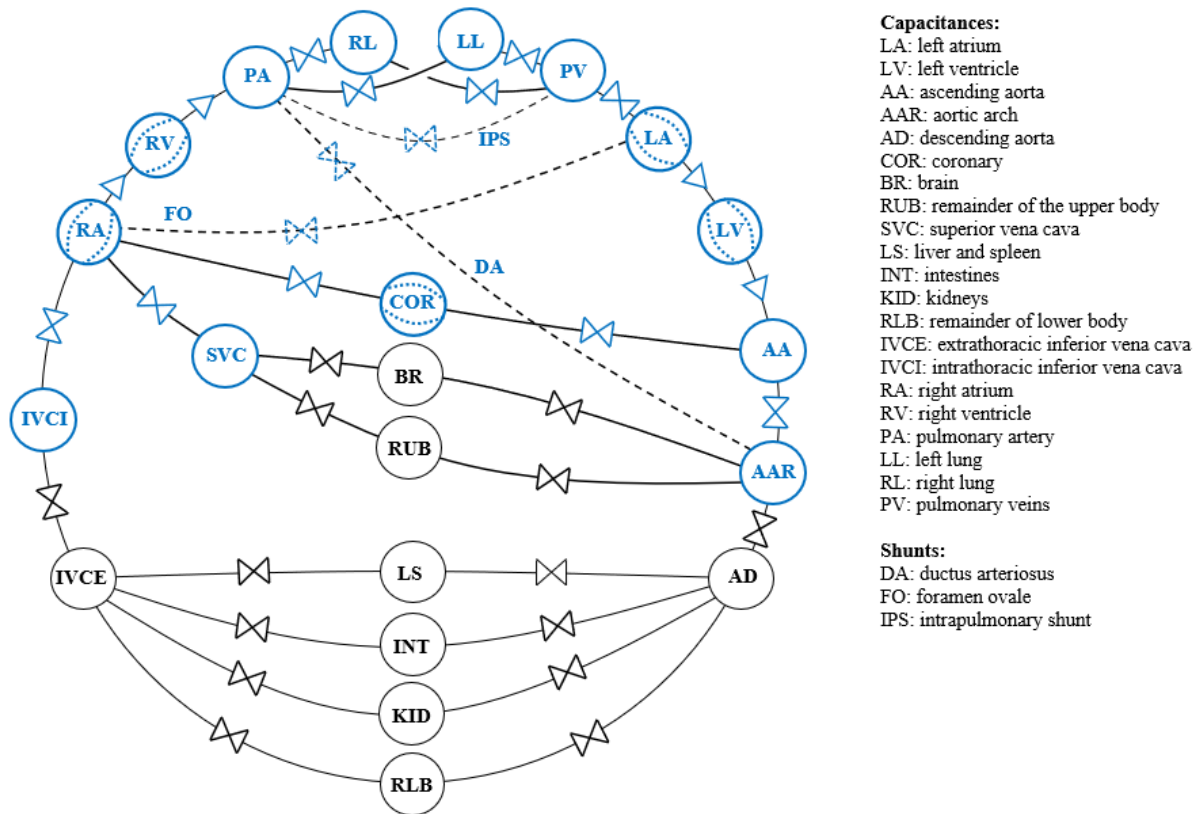
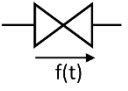
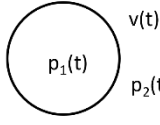
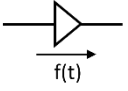
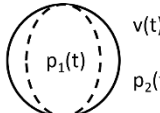


Figure A: Hydraulic circuit representation of neonatal hemodynamics. See Table A for used symbols. Intrathoracic components are indicated in blue and extra-thoracic components in black. Dashed lines and components represent shunts that are exclusive to the neonate, or more significant than in a typical adult.

Table A: Circuit elements. Volume $v(t)$, pressure $p(t)$, and flow rate $f(t)$.

Name	Symbol
Resistor	$p_1(t)$ —  — $p_2(t)$
Capacitance	 $v(t)$ $p_1(t)$ $p_2(t)$
Valve	$p_1(t)$ —  — $p_2(t)$
Time-varying elastance	 $v(t)$ $p_1(t)$ $p_2(t)$

Appendix B

Parameter values for the physiological situation.

Table A. Lymphatic model parameters UV in L, and E or E_{min} in mmHg/L for the capacitances and time-varying elastances respectively.

	UV	E or E_{min}
IS	0.9	1000
IL	0.006	5000
LT	0.005	5000
LD	0.005	9500

Table B. Lymphatic model parameter R in mmHg·s/L for the valves.

<i>From, to</i>	R
IS, IL	50
IL, LT	500
LT, LD	1500
LD, SVC	1500

Values for UV , E , E_{min} , and R were initially chosen in the same order of magnitude as for the blood capacitances of Explain. Based on simulations the values were changed to obtain the target values for IS pressure and LD outflow.

Lymphatic model parameters L_p , in cm/min·mmHg, S in cm², and σ , for the resistors. The parameter values are the same for all resistors in the lymphatics model. $L_p = 9.788 \cdot 10^{-10}$ cm/min·mmHg, $S = 50$ cm² and $\sigma = 0.7$. Initial values were chosen based on the literature. Then the values were changes based on the simulations to obtain an IS inflow equal to the target value for LD outflow.

The osmotic pressure in the lymph-containing components is calculated using the following parameters: $i = 1$, $R = 0.08206$ L·atm/mol·K, $T = 37$ degrees Celsius, $M = 0.09 \cdot 10^{-3}$ mol/L.

Table C. Parameter values for the feedback mechanism model.

	CV_{sp}	CV_{min}	CV_{max}	$g_{cv,low}$	$g_{cv,high}$
f in ml/min	0.1369	0	0.2783	-986121	-328707
p_{tm} in mmHg	9.65	7.65	11.65	22500	67500

Values for CV_{sp} were derived from the literature as described in Section 4.1. Values for CV_{min} and CV_{max} were chosen based on the simulations.

The lower and higher gains were calculated using the following equations:

$$me_{max}(a) = me_{ref} + [a(CV_{max}) \cdot g_{cv,high}],$$

and

$$me_{min}(a) = me_{ref} + [a(CV_{min}) \cdot g_{cv,low}].$$

$me_{ref} = 45000$ mmHg/ml·min, $me_{max} = 180\ 000$ mmHg/ml·min, and $me_{min} = 0$ in mmHg/ml·min

$tc = 3$ s. tc was chosen in the same order of magnitude as the time constant used for the response of the autonomic nerve system in Explain.

T_c (intrinsic pump) = 2 s. Based on the literature¹⁸.

R is calculated using Equation 21, filling in the maximum values for $freq$ (20 min^{-1} , chosen based on the literature) and me . Therefore, $R = 450 \text{ mmHg}\cdot\text{min}/\text{ml}$.